Supporting Information

Sulfonic Acid Functionalized Graphitic Carbon Nitride as Solid Acid-Base Bifunctional Catalyst for Knoevenagel Condensation and Multicomponent Tandem Reactions

Priyanka Choudhary,[1] Arghya Sen,[1,3] Ajay Kumar,[1] Suman Dhingra,[2]
C. M. Nagaraja,[2] and Venkata Krishnan[1]*

[1]School of Basic Sciences and Advanced Materials Research Center, Indian Institute of Technology Mandi, Mandi 175075, Himachal Pradesh, India. Email: vkn@iitmandi.ac.in

[2]Department of Chemistry, Indian Institute of Technology Ropar, Rupnagar 140001, India.

[3]Current address: Department of Chemistry, Indian Institute of Technology Kanpur, Kalyanpur, Kanpur 208016, India.

Sl. No.	Contents	Page No.
1	Chemicals	S-3
2	Materials characterization	S-4
3	**Fig. S1** PXRD patterns g-C_3N_4 and different S-g-C_3N_4 catalysts	S-5
4	**Fig. S2** SEM images of (a, b) g-C_3N_4 nanosheets and (c, d) S-g-C_3N_4 nanosheets	S-6
5	**Fig. S3** Survey spectra of g-C_3N_4 and S-g-C_3N_4 nanosheets	S-7
6	**Table S1** Atomic percentage of elements in different catalysts from XPS analysis	S-7
7	Product yield calculation	S-8
8	Calculation of number of active sites and turnover number (TON)	S-9
9	Green metrics calculations	S-10
10	**Table S2** Summary of green metrics parameters for Knoevenagel condensation reactions	S-11
11	**Table S3** Summary of green metrics parameters for sequential tandem reactions	S-12
12	**Table S4** Variation of different S-g-C_3N_4 catalysts used for Knoevenagel condensation model reaction	S-13
13	**Table S5** Optimization catalyst amount of for Knoevenagel condensation reaction	S-14

14	**Table S6** Optimization catalyst amount for sequential tandem reaction	S-14
15	**Table S7** Comparison of previously reported catalyst for Knoevenagel condensation reaction.	S-15
16	**Table S8** Comparison of previously reported catalyst for multicomponent sequential tandem reaction.	S-16
17	**Fig. S4** Survey spectra of fresh and recycled S-g-C_3N_4 (after five cycles) catalysts.	S-18
18	**Table S9** Atomic percentage of elements in fresh and recycled S-g-C_3N_4 catalysts (after five cycles) obtained from XPS analysis.	S-18
19	NMR spectra of the obtained compounds	S-19
20	References	S-35

S1. Chemicals

Dicyandiamide (99%, Sigma Aldrich), chlorosulphuric acid (≥97% Merck), dimethyl carbonate (99%, Alfa Aesar), ethanol (≥99.5%, Merck), dichloromethane (99%, Fischer Scientific), isopropyl alcohol (99.5%, Sisco Research), hexane (Fischer Scientific) and ethyl acetate (Merck) were bought and used without any further purification. Deionized water (18.2 MΩ cm) was obtained from a double stage water purifier (ELGA PURELAB Option-R7).

S2. Materials characterization

The detailed characterization of catalysts was performed by using various instruments. The powder X-ray diffraction data was collected using a Rigaku SmartLab 9 kW rotating anode X-ray diffractometer in a Bragg−Brentano configuration using a Cu-sealed tube (Cu K_α X-rays of 0.1541 nm) operating at 45 kV and 100 mA. The measurements were performed in the scattering 2θ range from 5^o to 80^o with a scan rate of 2^o per min and a step size of 0.02^o. Raman spectroscopy measurements were done on Horiba LabRaM high resolution instrument using 785 nm laser excitation. FT-IR measurements were done on Agilent K8002AA Cary 660 instrument. Thermogravimetric analysis (TGA) was performed using a PerkinElmer Pyris 1 instrument. The samples were heated under a nitrogen atmosphere from 25 ^{o}C to 750 ^{o}C with the heating rate of 10 ^{o}C min^{-1} at a flow rate of 20 mL min^{-1}. The morphological analysis was done using a scanning electron microscope (SEM) FEI Nova SEM-450 and transmission electron microscope (TEM) FEI Tecnai G2 20 S-twin microscope operating at 200 kV. Energy dispersive analysis of X-ray (EDAX) spectrum and elemental mapping data were also obtained by using the same TEM instrument. The X-ray photoelectron spectroscopy (XPS) measurements were done using Thermo Scientific NEXSA photoemission spectrometer using Al-Kα (1486.6 eV) X-rays. The XPS data were acquired with a spot size 400 µm having a standard lens mode. The obtained data from the instrument were plotted and deconvoluted using Avantage software. The Brunauer–Emmett–Teller (BET) specific surface area was measured on Quanta chrome Autosorb-iQ-MP-XR system at 77 K. The temperature-programmed desorption (TPD) study was done using CHEMBET™ TPR/TPD, QUANTACHROME. NMR spectra were measured using a JEOL-USA (JNMECX500) spectrometer in DMSO-d_6 using TMS (tetramethyl silane) as an internal standard. The ^{1}H and ^{13}C chemical shifts in NMR is reported in ppm relative to 7.26 and 77.23 of the $CDCl_3$ solvent as the standard. The coupling constant “J” was calculated in Hz. All ^{1}H-NMR spectra were recorded at 500 MHz frequency, wherein ^{13}C-NMR spectra were recorded at 125 MHz frequency.

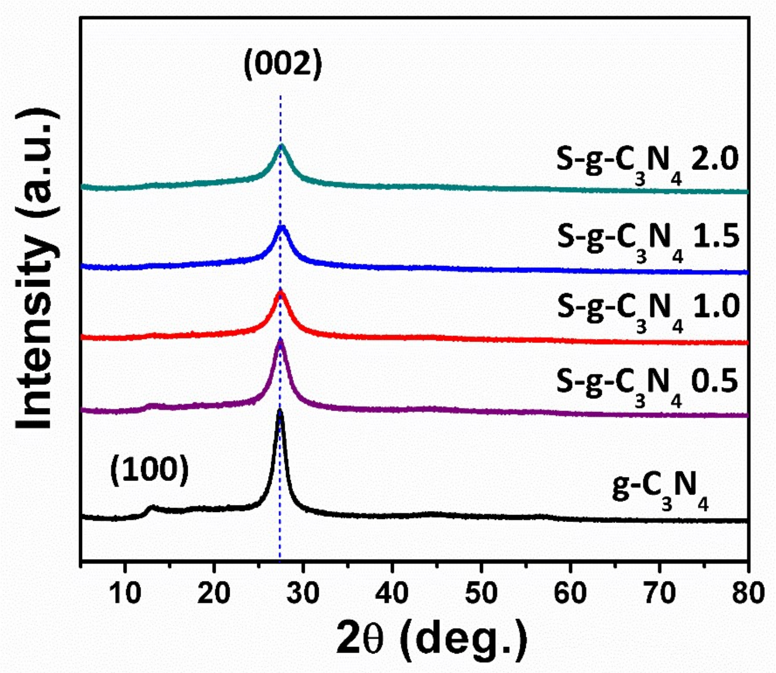

Fig. S1 PXRD patterns g-C_3N_4 and different S-g-C_3N_4 catalysts.

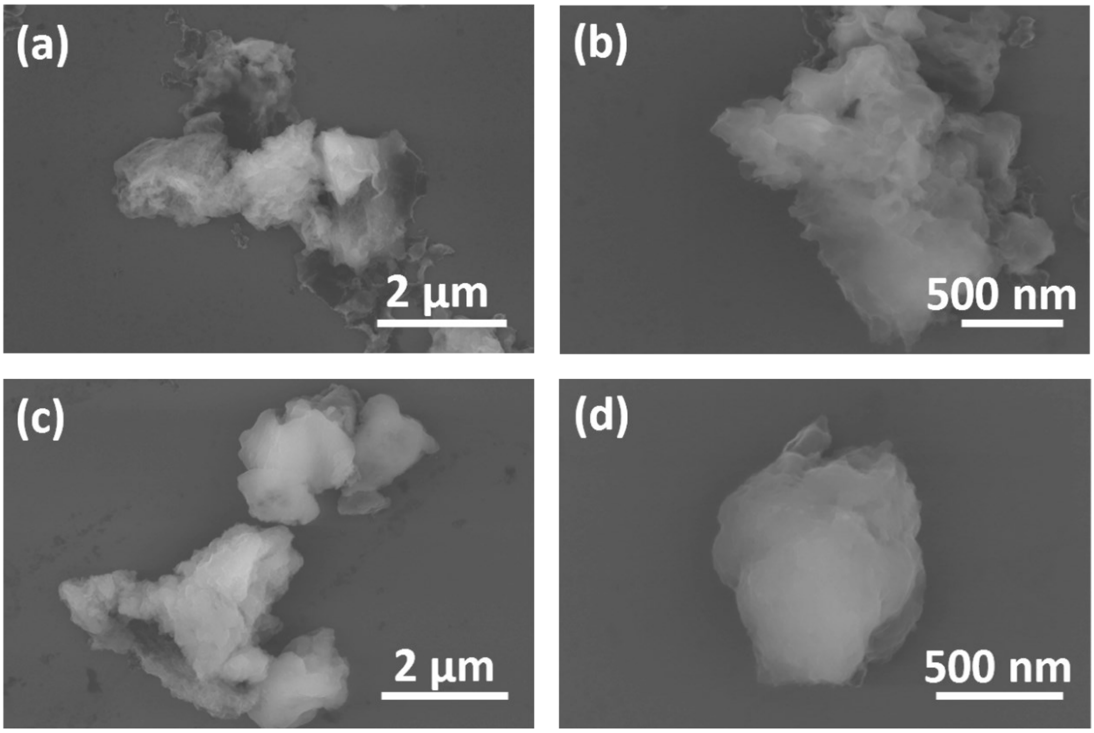

Fig. S2 SEM images of (a, b) g-C_3N_4 nanosheets and (c, d) S-g-C_3N_4 nanosheets.

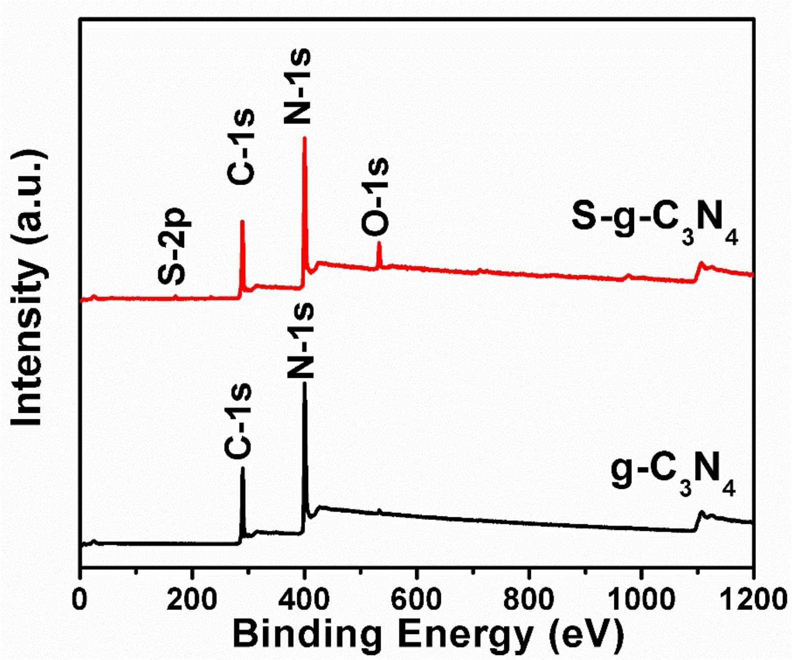

Fig. S3 Survey spectra of g-C_3N_4 and S-g-C_3N_4 nanosheets.

Table S1 Atomic percentage of elements in different catalysts from XPS analysis.

Sl. No.	Catalyst	Atomic percentage of constituent elements			
		C-1s	**N-1s**	**O-1s**	**S-2p**
1	g-C_3N_4	41.22	58.78	-	-
2	S-g-C_3N_4 0.5	42.28	47.79	9.50	0.44
3	S-g-C_3N_4 1.0	40.28	52.58	6.40	0.74
4	S-g-C_3N_4 1.5	44.65	46.27	7.55	1.52
5	S-g-C_3N_4 2.0	41.94	43.65	12.64	1.77

S3. Product yield calculation:

The product yield was calculated after purification of the product using column chromatography. The yield of the product was calculated by using the following formula:

$$Yield\ (\%) = \frac{Actual\ yield\ (in\ mg)}{Theoretical\ yield\ (in\ mg)} \times 100$$

Herein, theoretical yield = Molecular weight of product × mmol of reactants (theoretical yield is the 100 % yield)

S4. Detailed calculation of number of active sites and turnover number (TON)

Active sites are referred to catalytically effective sites which can perform the required reaction. The Turnover number (TON) describes the effectiveness of the as synthesized catalyst for a particular reaction. It can be calculated as below:

$$TON = \frac{(\%\text{conversion}) \times \text{No. moles of reactants}}{\text{No. of moles of catalyst}}$$

From the TPD analysis of S-g-C_3N_4 nanosheets it was found that:

Amount of acidic sites = 0.147 mmol g^{-1}

Amount of basic sites = 0.097 mmol g^{-1}

Since the both acid and base sites act as active sites for our catalytic system hence,

Total number of active sites = 0.244 mmol g^{-1}

Since, according to TPD analysis, 1 g of catalyst = 0.244 mmol of active sites.

Therefore, 1 mg of catalyst = 2.44 $\times$ 10^{-3} mmol of active sites.

For Knoevenagel condensation 20 mg of S-g-C_3N_4 catalyst was used;

20 mg of catalyst = 4.88 $\times$ 10^{-2} mmol of active sites.

For Tandem reactions 30 mg of S-g-C_3N_4 catalyst was used;

30 mg of catalyst = 7.2 $\times$ 10^{-2} mmol of active sites.

For the Knoevenagel condensation model reaction involving 4-nitrobenzaldehyde and malononitrile, TON can be calculated as below:

$$TON = \frac{94 \times 2}{4.88 \times 10^{-2}}$$

TON = 3916

Similarly, TON for all the reactions was calculated and is given in Table 2 and Table 3 in the main manuscript.

S5. Green metrics calculations

Green metrics parameters describe the environmental impact and sustainability of the reactions. Different green metrics parameters were calculated for the developed Knoevenagel condensation and sequential tandem reactions as discussed below.

(1) Environmental factor (E-factor): E-factor defines the ratio of mass of waste to mass of product. It implies how much waste is generated in a chemical process. For an ideal Green chemical reaction, E-factor should be 0. Higher the E-factor means more amount of waste is generated which can have a detrimental impact on environment.

$$E - factor\ =\ (mass\ of\ waste)/(mass\ of\ product)$$

$$Mass\ of\ waste\ =\ Total\ mass\ of\ raw\ materials\ -\ Total\ mass\ of\ product$$

(2) Atom economy (AE): AE of a reaction describes the total number of atoms resides in the product from the starting materials. It determines the efficiency of a reaction. The ideal value of AE factor is 100%.

$$AE\ =\ Mol.\ wt.\ of\ product/\ \Sigma(Mol.\ wt.\ of\ stoichiometric\ reactants)\ \times\ 100$$

(3) Mass intensity (MI): MI is the total mass involves in process divided by the mass of product. Lower the mass intensity value, lower will be the cost and the process will be more sustainable.

$$MI\ = (Total\ mass\ in\ process)\ /\ (Mass\ of\ product)$$

(4) Process mass intensity (PMI): PMI is the total mass used in a chemical process including the mass of the solvents used divided by the mass of product.

$$PMI\ =\ [Total\ mass\ in\ process\ (including\ solvent)]\ /\ [Mass\ of\ product]$$

(5) Reaction mass efficiency (RME): Reaction mass efficiency is defined as the mass of product divided by the sum of total mass of stoichiometric reactants. RME measures the “cleanness” of a chemical reaction. Values of RME range from 0-100%. Higher value of RME is considered better for an ideal green chemical reaction.

$$RME\ (\%)\ =\ mass\ of\ product\ /\Sigma(mass\ of\ stoichiometric\ reactants)\ \times\ 100$$

Table S2 Summary of green metrics parameters calculated for the Knoevenagel condensation.

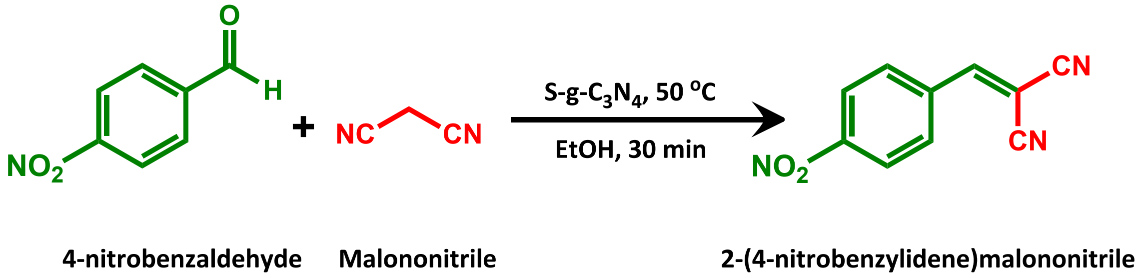

Sl. No.	Green metrics parameters	Calculated values
1	Environmental factor (E-factor)	0.064
2	Atom economy (AE)	91.5 %
3	Mass intensity (MI)	1.064
4	Process mass intensity (PMI)	1.517
5	Reaction mass efficiency (RME)	93.9 %

Table S3 Summary of green metrics parameters calculated for the sequential tandem reaction.

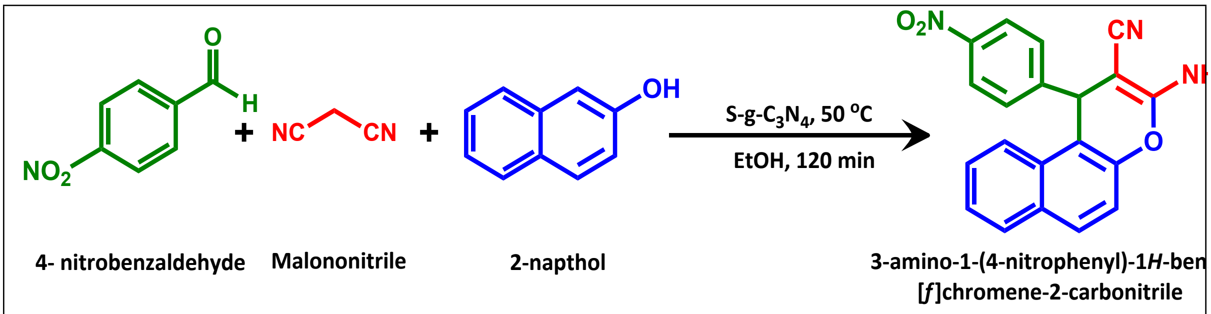

Sl. No.	Green metric parameters	Calculated values
1	Environmental factor (E-factor)	0.086
2	Atom economy (AE)	94.9 %
3	Mass intensity (MI)	1.086
4	Process mass intensity (PMI)	1.363
5	Reaction mass efficiency (RME)	92.1 %

Table S4 Different S-g-C_3N_4 catalysts used for Knoevenagel condensation model reaction.

Sl. No.	**Catalyst**	**Amount of catalyst (mg)**	**Temperature (^oC)**	**Time (min)**	**Yield (%)**
1	S-g-C_3N_4 0.5	20	50	30	78
2	S-g-C_3N_4 1.0	20	50	30	94
3	S-g-C_3N_4 1.5	20	50	30	87
4	S-g-C_3N_4 2.0	20	50	30	82

Table S5 Optimization of S-g-C_3N_4 catalyst amount for Knoevenagel condensation.

Sl. No.	**Catalyst**	**Amount of catalyst (mg)**	**Temperature (^oC)**	**Time (min)**	**Yield (%)**
1	S-g-C_3N_4	10	RT	60	56
2	S-g-C_3N_4	20	RT	60	78
3	S-g-C_3N_4	20	50	30	82
4	S-g-C_3N_4	20	50	60	92
5	S-g-C_3N_4	30	50	30	92

Table S6 Optimization of S-GCN catalyst amount for sequential tandem reaction.

Sl. No.	**Catalyst**	**Amount of catalyst (mg)**	**Temperature (^oC)**	**Time (min)**	**Yield (%)**
1	S-g-C_3N_4	10	50	60	45
2	S-g-C_3N_4	20	50	60	64
3	S-g-C_3N_4	20	50	120	78
4	S-g-C_3N_4	30	50	120	92
5	S-g-C_3N_4	40	50	120	94

Table S7 Comparison of previously reported catalyst for Knoevenagel condensation reaction.

Sl. No.	**Catalyst**	**Temperature (^oC)**	**Solvent**	**Time (min)**	**Yield (%)**	**Reference**
1	$HoCrO_4$	33 ^oC	H_2O	20	92	1
2	Fe NP's/Am@rGO	40 ^oC	Toulene	180	100	2
3	CS-CA/Cu-MOF	25 ^oC	Solvent free	15	100	3
4	V-Zn-MOF	60 ^oC	Solvent free	60	99	4
5	NUC-25	80 ^oC	MeOH	1440	99	5
6	Amino functionalized Zn/Cd-MOF	60 ^oC	Solvent free	360	99.9	6
7	$SrTiO_3$	75 ^oC	EtOH or H_2O	360	100	7
8	Chitosan	40 ^oC	EtOH	360	100	8
9	Fe_3O_4@SiO_2	75 ^oC	Toulene	45	100	9
10	TiO_2 NP's	75 ^oC	EtOh	30	99	10
11	Hf(IV) MOF	RT	EtOH	240	99	11
12	S-g-C_3N_4	50 ^oC	EtOH	30	94	This work
NP's- Nanoparticles, MOF – Metal organic framework, Fe NP's/Am@rGO – Fe nanoparticles decorated amino-modified reduced graphene oxide, CS-CA/Cu-MOF - Cu-MOF immobilized modified chitosan metal organic framework, V-Zn-MOF - Zn(bix)]{V_2O_6}, NUC-25 - {(Me_2NH_2)[$Tm_3(BDCP)_2)(H_2O)_3$]· 4DMF·H_2O}$_n$.						

Table S8 Comparison of previously reported catalyst for multicomponent sequential tandem reaction.

Sl. No.	Catalyst	Temperature	Solvent	Time (min)	Yield (%)	Reference
1	PANF	80 °C	H_2O	60	95	12
2	Bi_2WO_6 NP's	RT	H_2O	20	88	13
3	$ZnFe_2O_4$	RT	H_2O	180	91	14
4	SBA-15-pr-bu-triazole-OH	Reflux	H_2O	300	93	15
5	ZnO NP's thin film	60 °C	H_2O	60	96	16
6	Zn(L-proline)$_2$	Reflux	EtOH	180	91	17
7	Fe_3O_4@SiO_2-Sultone	60 °C	Solvent free	25	97	18
8	CuO-ZnO	Reflux	H_2O	18	92	19
9	Ni–Al_2O_3	Reflux	EtOH/ H_2O (1:1)	80	82	20
10	SBA-15@methenamine-HPA	Reflux	H_2O	15	92	21
11	Z-HY@SiO_2-Pr-Py	Reflux	Solvent free	90	95	22
12	piperazine-GO	100 °C	Solvent free	30	97	23
13	SiO_2@Im-Fc[OAc]	90 °C	Solvent free	35	90	24
14	PIL-SB Mn-(III)	80 °C	H_2O	15	95	25
15	ZrO_2	80 °C	H_2O	45	92	26
16	Fe_3O_4	80 °C	Solvent free	25	89	27
17	S-g-C_3N_4	50 °C	EtOH	120	92	This work

PANF - Prolinamide functionalized polyacrylonitrile fiber, Fe_3O_4@PS-Arg -

Fe_3O_4@propylsilan-arginine, SBA-15-pr-bu-triazole-OH - propyl triazole functionalized SBA-15, HPA - heteropolyacids, Z-HY@SiO_2-Pr-Py - alkylaminipyridine-grafted HY Zeolite, GO - Graphene oxide, SiO_2@Im-Fc[OAc] - silica nanospheres containing ferrocene-tagged imidazolium acetate, PIL-SB Mn-(III) - polymeric imidazolium ionic liquid functionalized Mn(III) Schiff base complex.

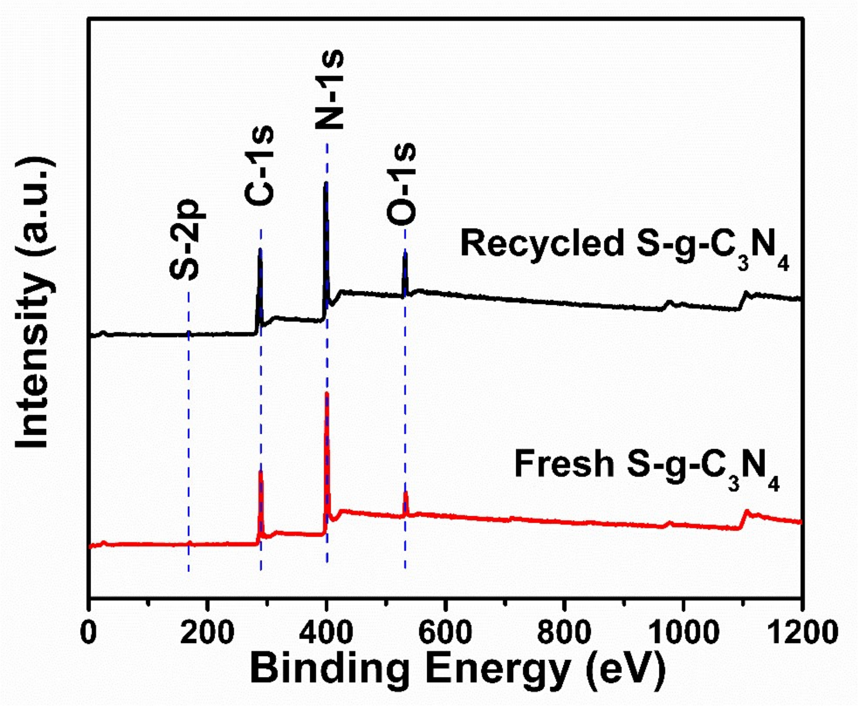

Fig. S3 Survey spectra of fresh and recycled S-g-C_3N_4 (after five cycles) catalysts.

Table S9 Atomic percentage of elements in fresh and recycled S-g-C_3N_4 catalysts (after five cycles) obtained from XPS analysis.

Sl. No.	**Elements**	**Atomic percentage (%)**	
		Fresh S-g-C_3N_4	**Recovered S-g-C_3N_4**
1	C-1s	40.28	40.26
2	N-1s	52.58	49.74
3	S-2p	0.74	0.57
4	O-1s	6.40	9.43

S6. NMR spectra of the compounds

^{1}H-NMR spectra of 2-benzylidenemalononitrile [500 MHz, $CDCl_3$]

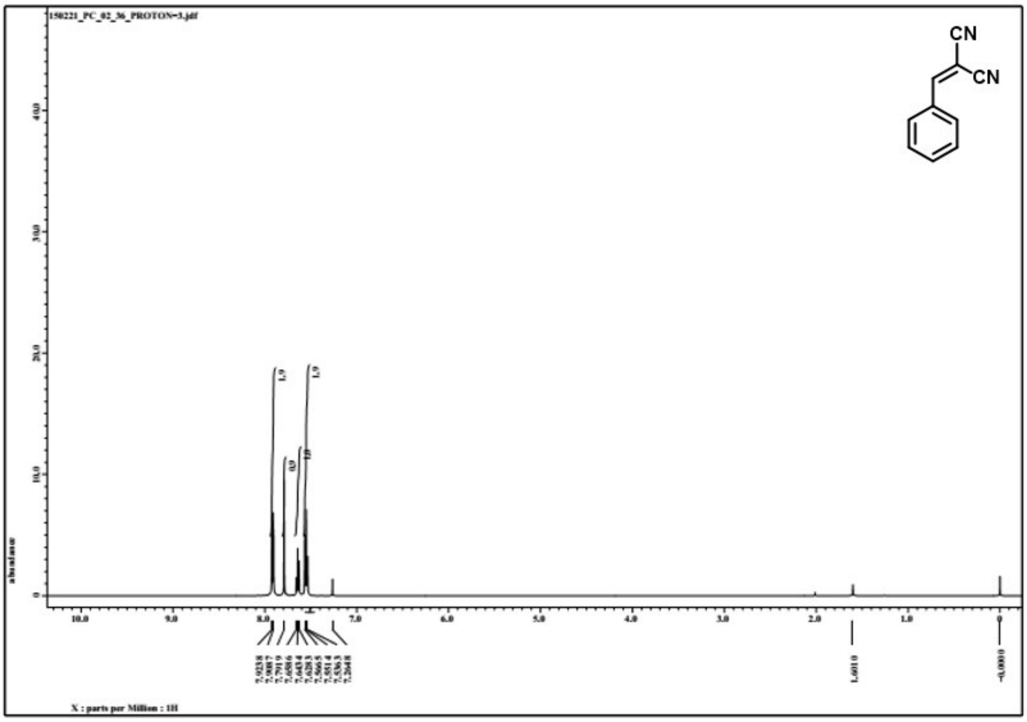

^{13}C-NMR spectra of 2-benzylidenemalononitrile [125 MHz, $CDCl_3$]

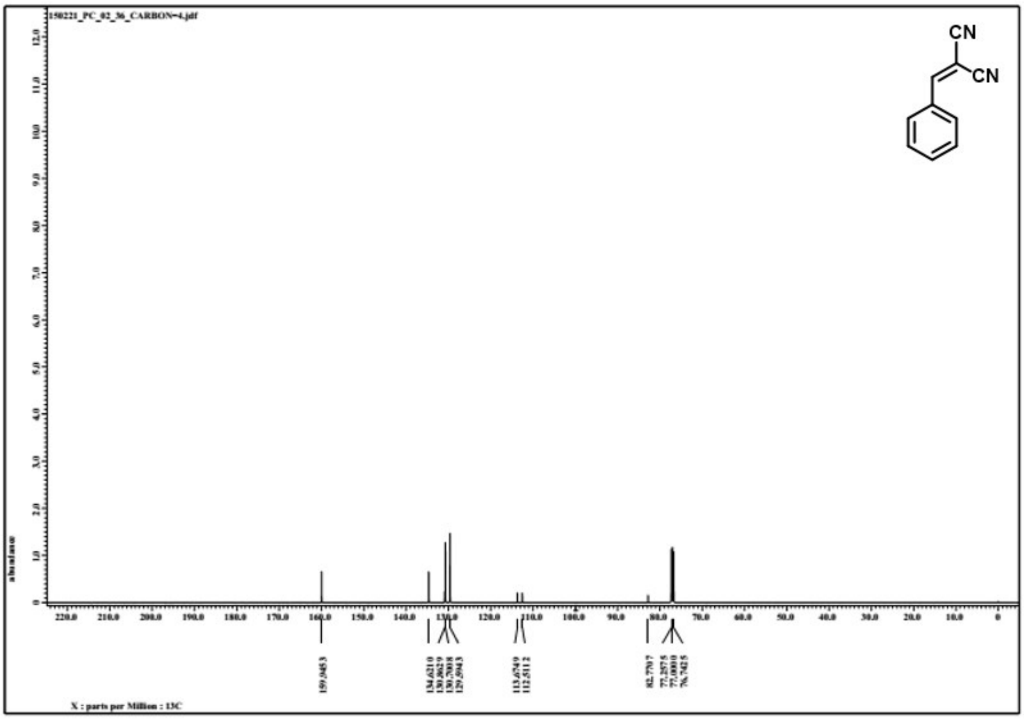

^{1}H-NMR spectra of 2-(4-chlorobenzylidene)malononitrile [500 MHz, $CDCl_3$]

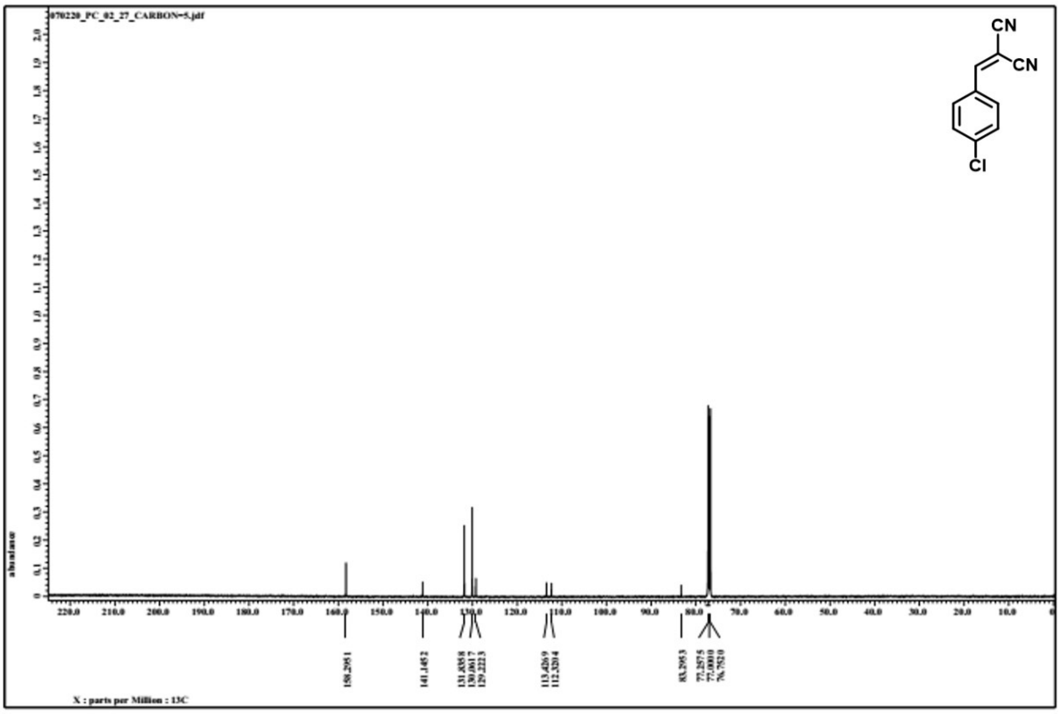

^{13}C-NMR spectra of 2-(4-chlorobenzylidene)malononitrile [125 MHz, $CDCl_3$]

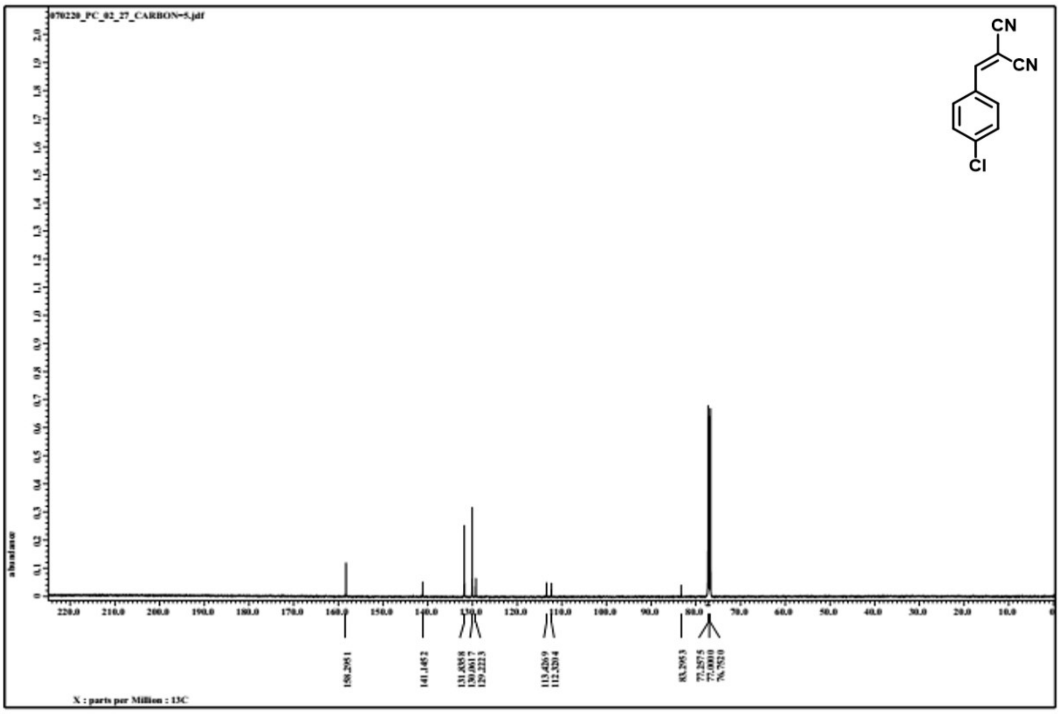

^{1}H-NMR spectra of 2-(4-nitrobenzylidene)malononitrile [500 MHz, $CDCl_3$]

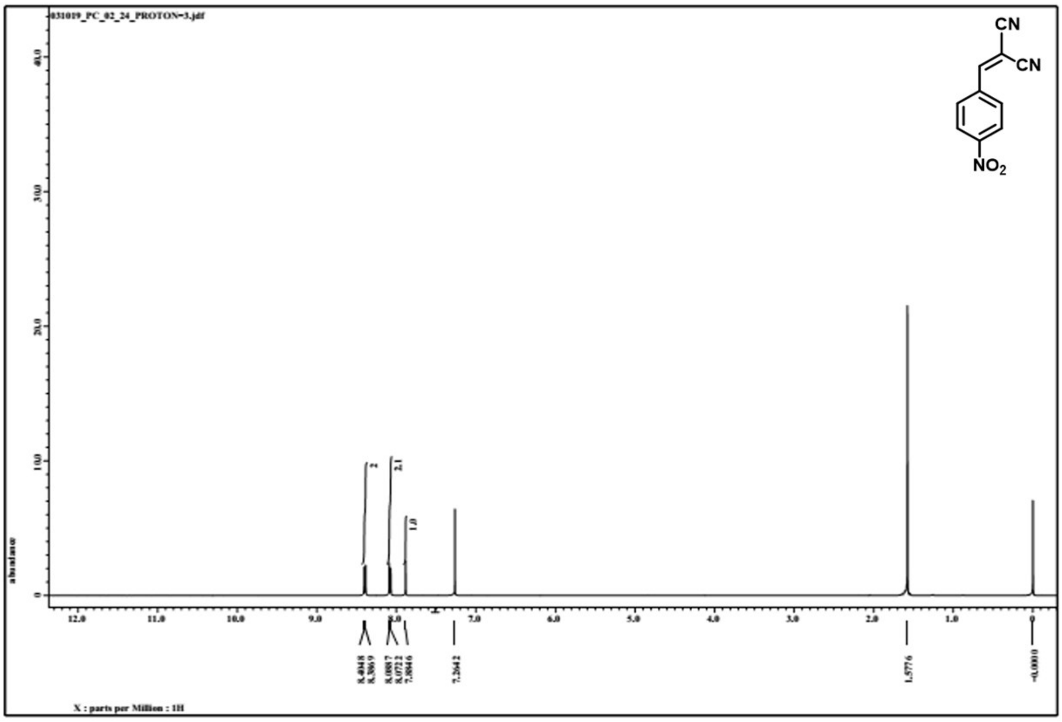

^{13}C-NMR spectra of 2-(4-nitrobenzylidene)malononitrile [125 MHz, $CDCl_3$]

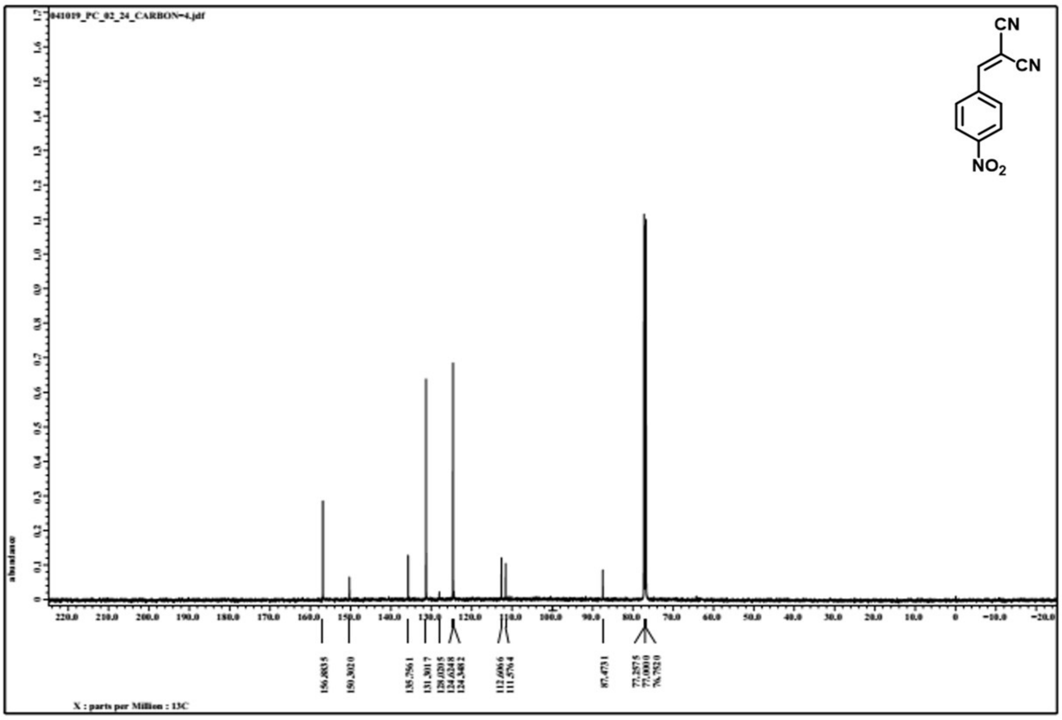

^{1}H-NMR spectra of 2-(4-methylbenzylidene)malononitrile [500 MHz, $CDCl_3$]

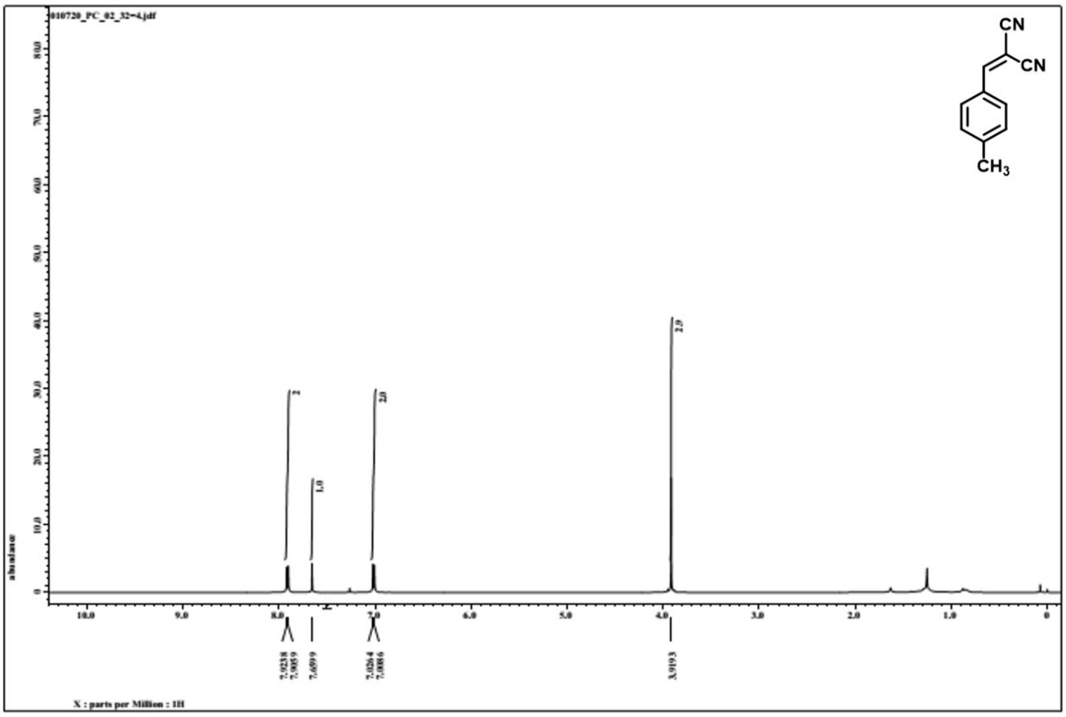

^{13}C-NMR spectra of 2-(4-methylbenzylidene)malononitrile [125 MHz, $CDCl_3$]

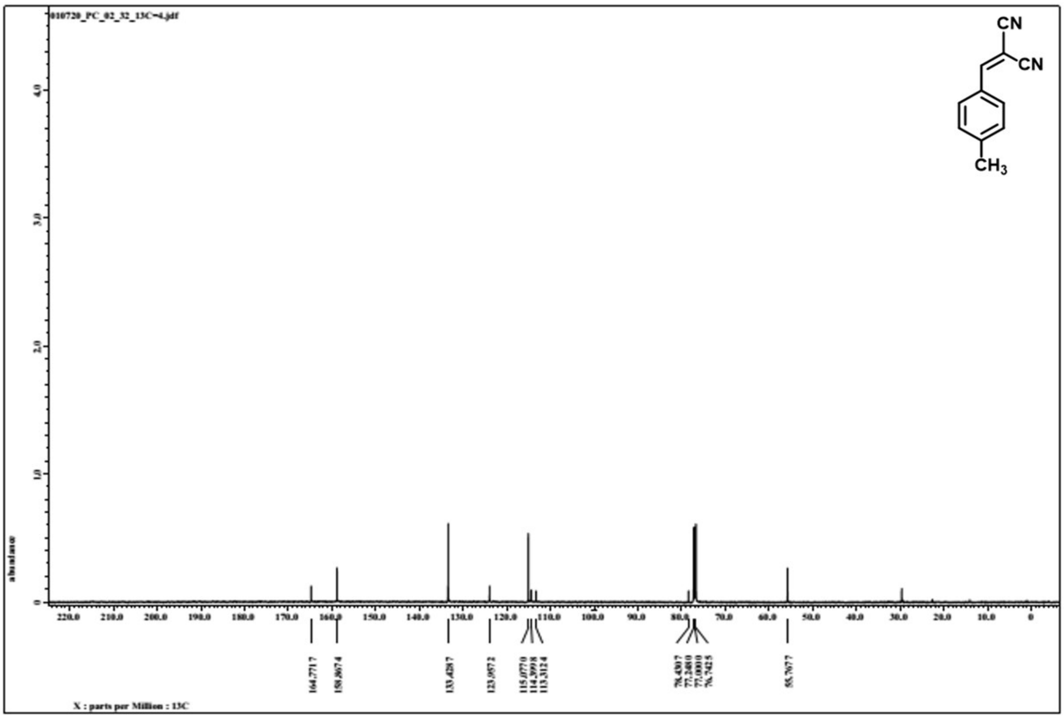

^{1}H-NMR spectra of 2-(4-(dimethylamino)benzylidene)malononitrile [500 MHz, $CDCl_3$]

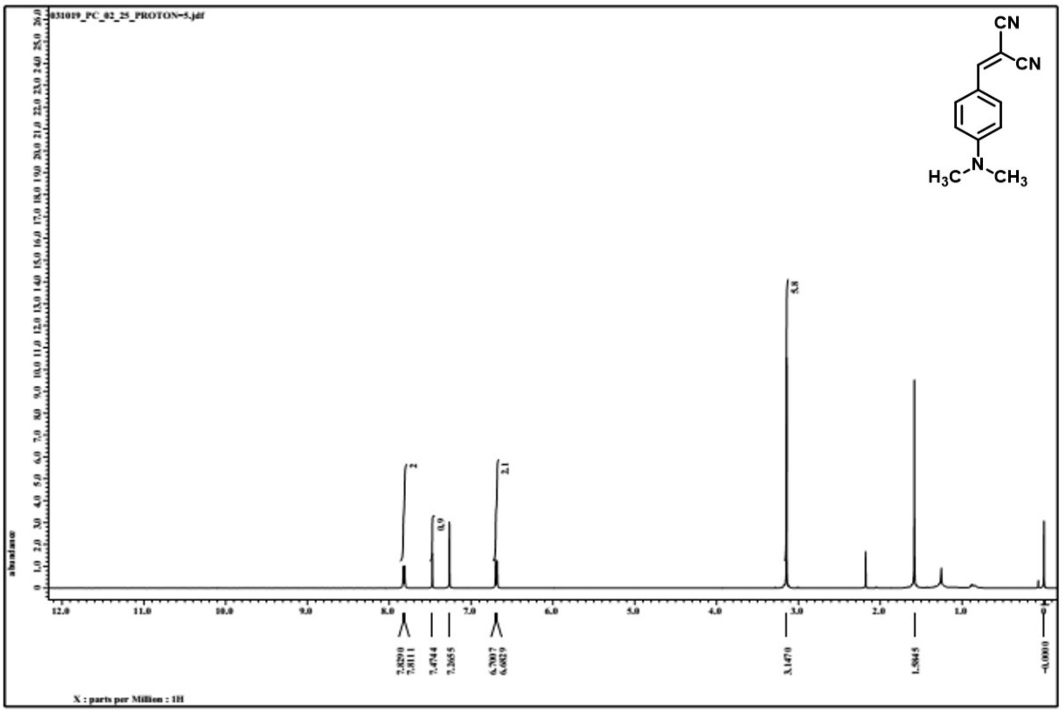

^{13}C-NMR spectra of 2-(4-(dimethylamino)benzylidene)malononitrile [125 MHz, $CDCl_3$]

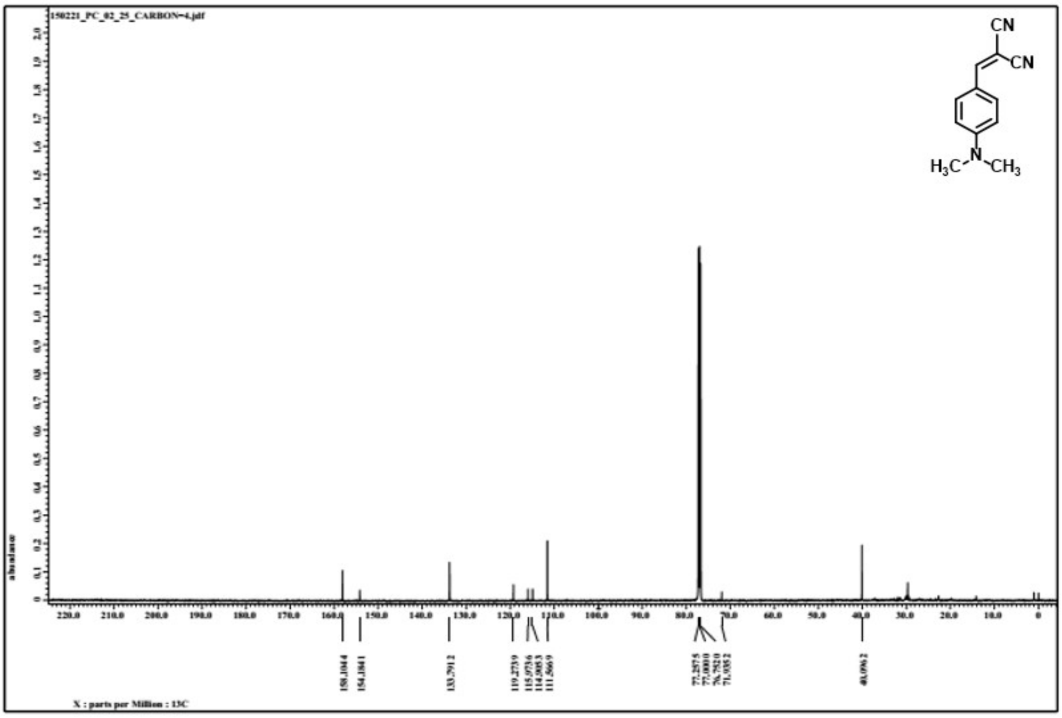

^{1}H-NMR spectra of 2-(4-methoxybenzylidene)malononitrile [500 MHz, $CDCl_3$]

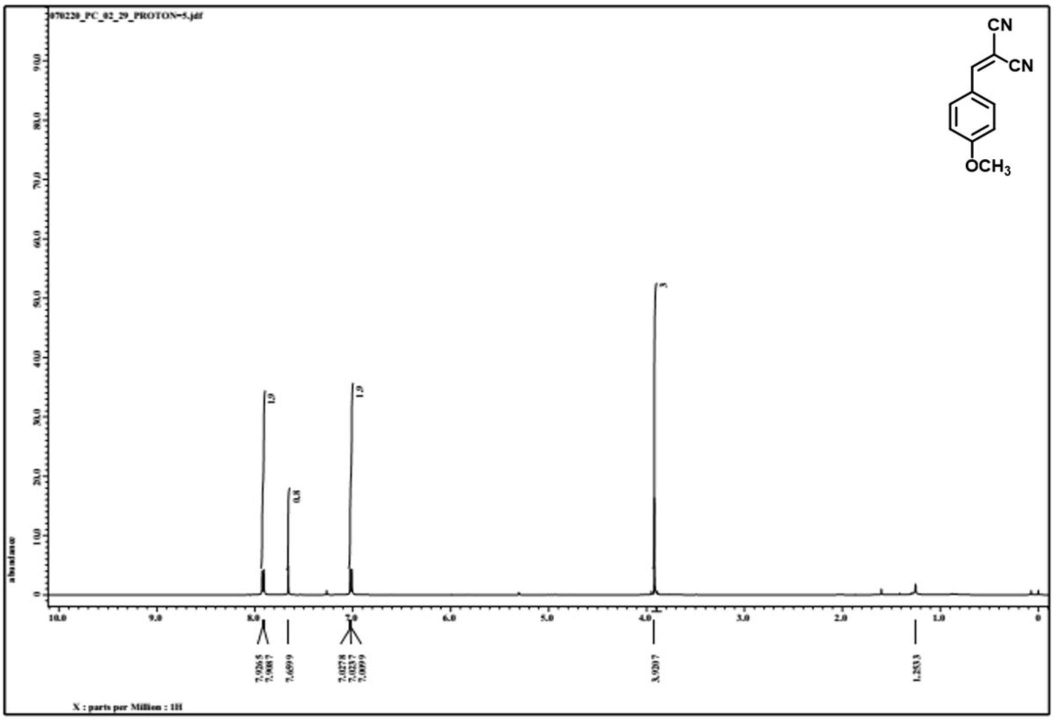

^{13}C-NMR spectra of 2-(4-methoxybenzylidene)malononitrile [125 MHz, $CDCl_3$]

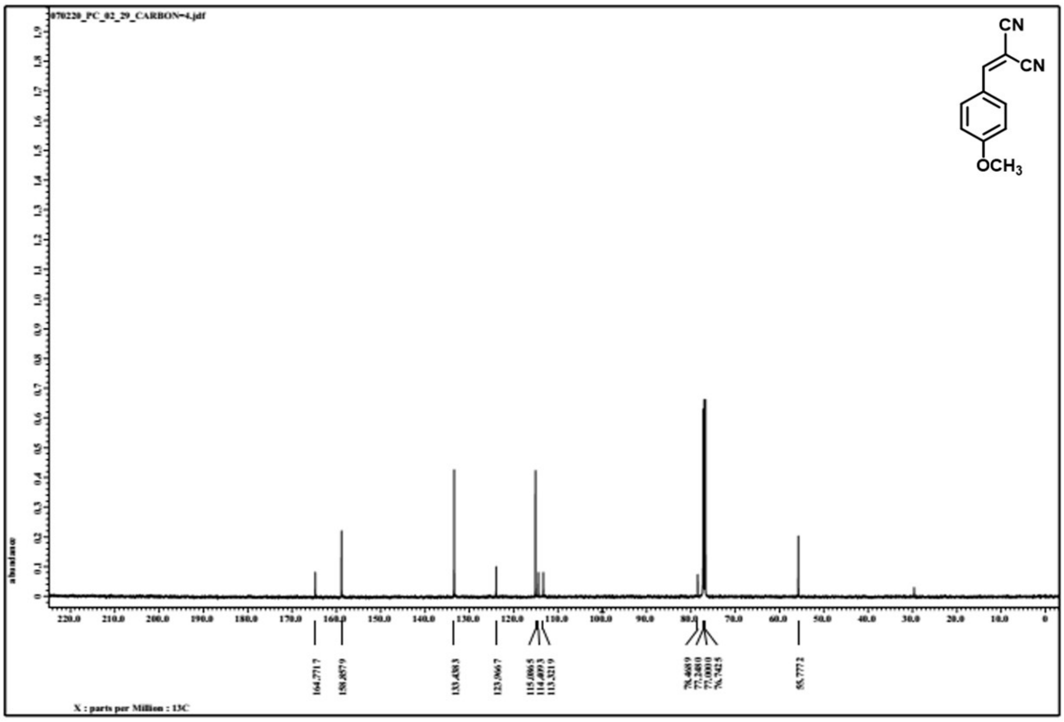

^{1}H-NMR spectra of 2-(2-methoxybenzylidene)malononitrile [500 MHz, CDCl$_3$]

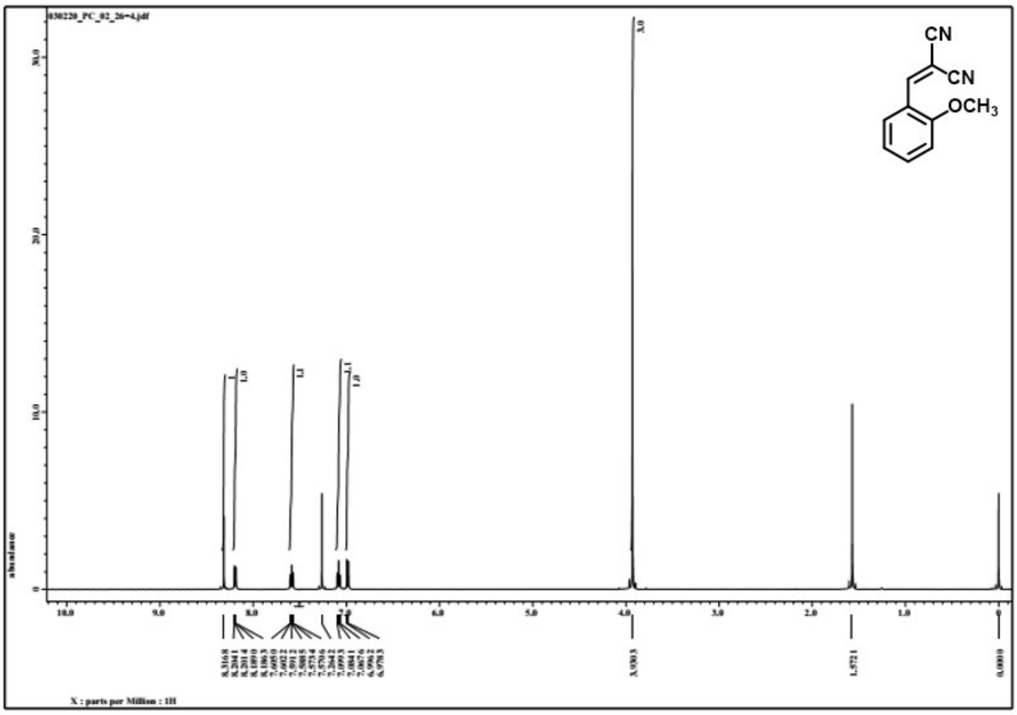

^{13}C-NMR spectra of 2-(2-methoxybenzylidene)malononitrile [125 MHz, CDCl$_3$]

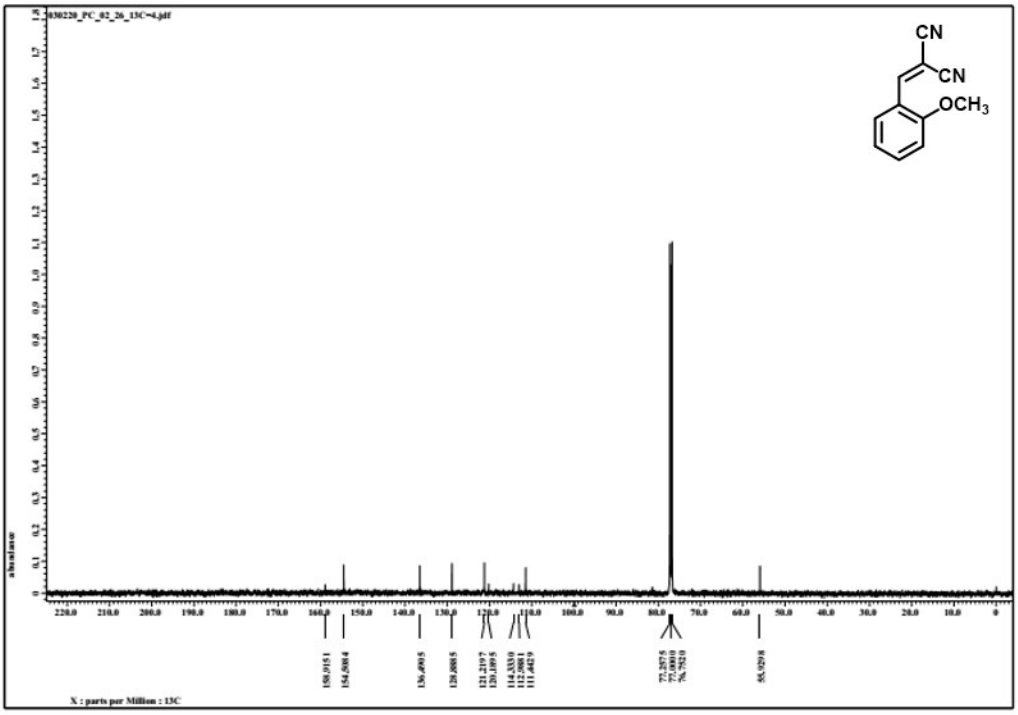

^{1}H-NMR spectra of 2-(2-nitrobenzylidene)malononitrile [500 MHz, $CDCl_3$]

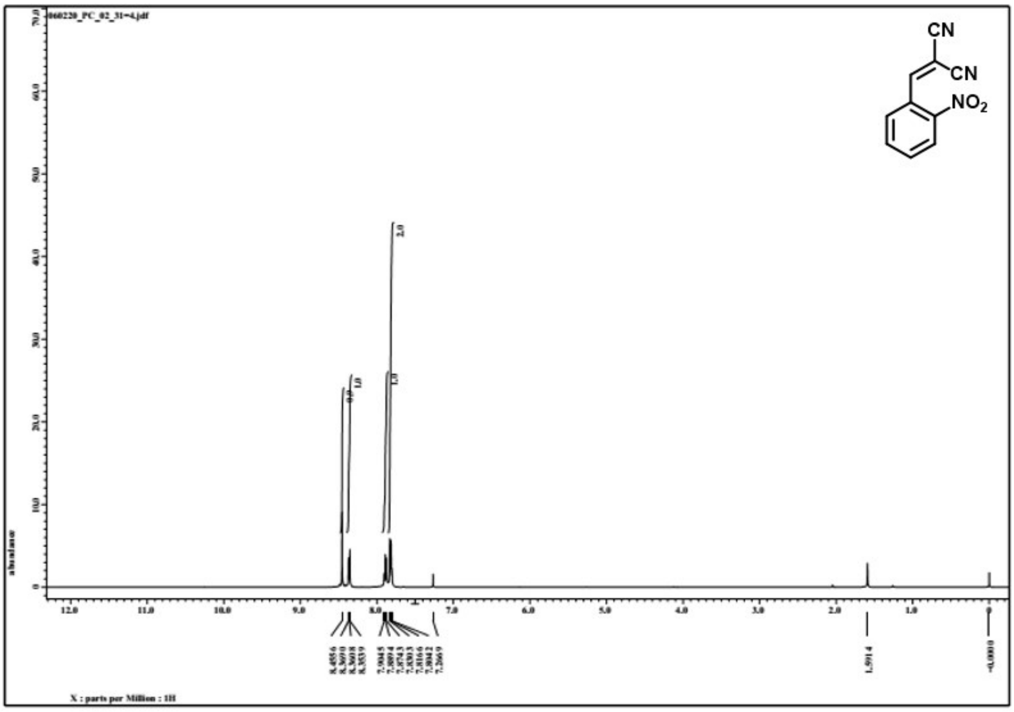

^{13}C-NMR spectra of 2-(2-nitrobenzylidene)malononitrile [125 MHz, $CDCl_3$]

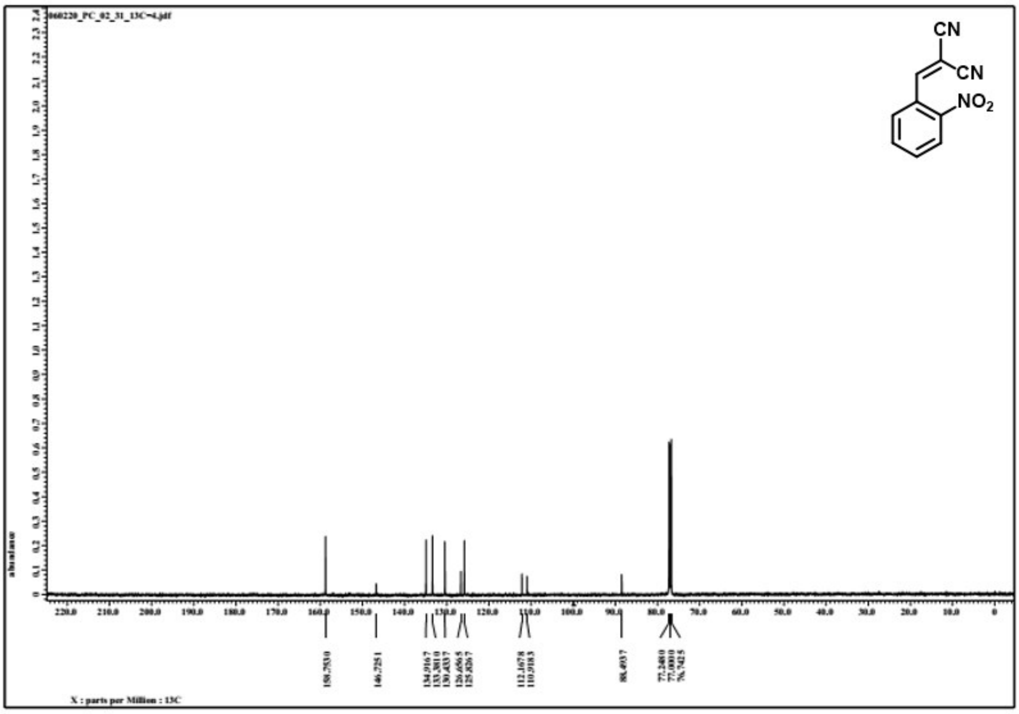

^{1}H-NMR spectra of 2-(3,5-dibromobenzylidene)malononitrile [500 MHz, $CDCl_3$]

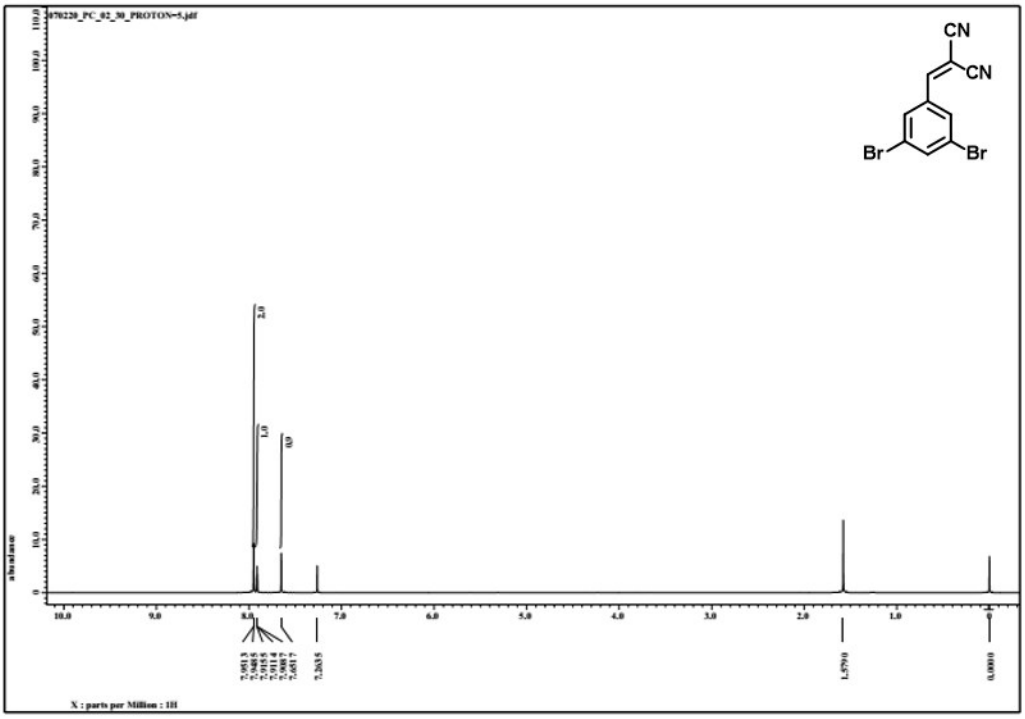

^{13}C-NMR spectra of 2-(3,5-dibromobenzylidene)malononitrile [125 MHz, $CDCl_3$]

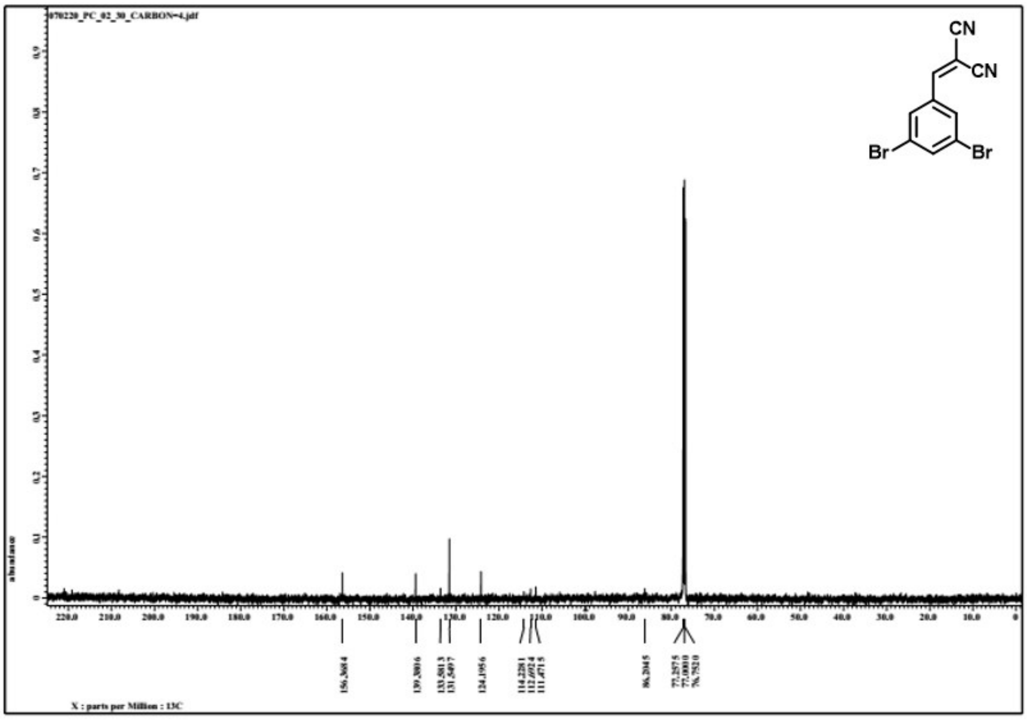

^{1}H-NMR spectra of Ethyl 2-cyano-3-(4-nitrophenyl)acrylate [500 MHz, CDCl$_3$]

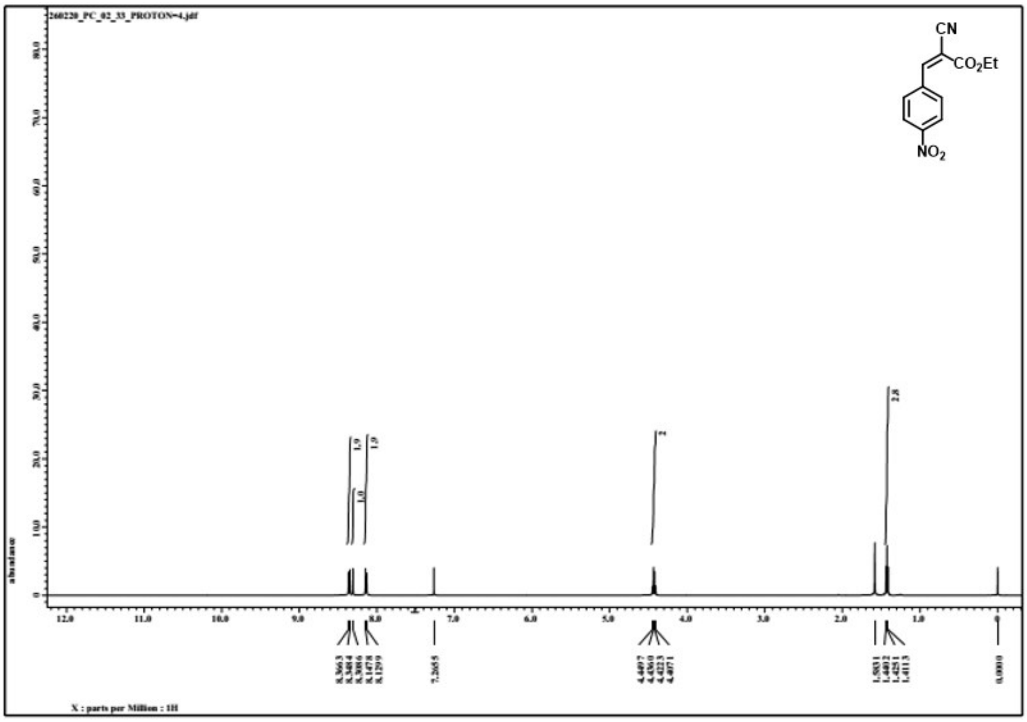

^{13}C-NMR spectra of Ethyl 2-cyano-3-(4-nitrophenyl)acrylate [125 MHz, CDCl$_3$]

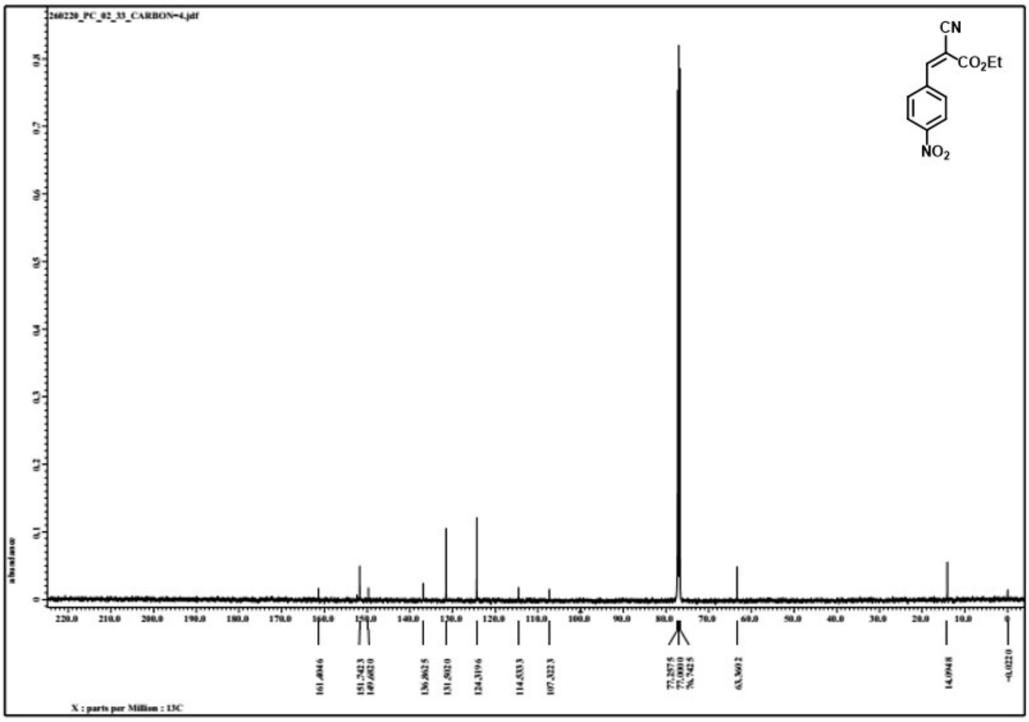

^{1}H-NMR spectra of 2-(thiophen-2-ylmethylene)malononitrile [500 MHz, $CDCl_3$]

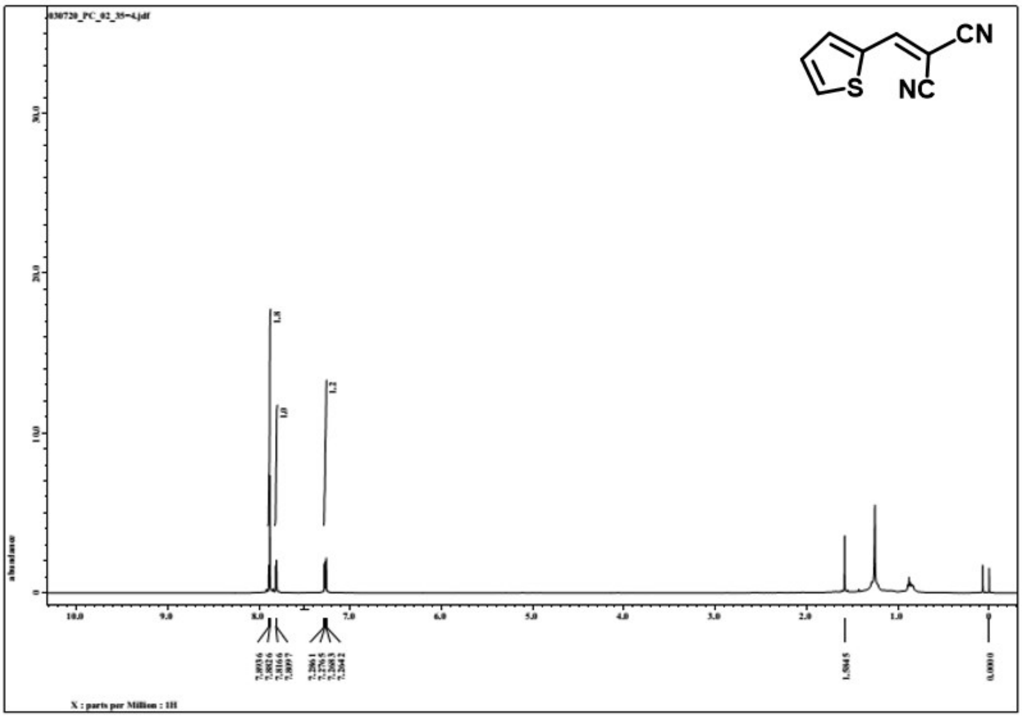

^{13}C-NMR spectra of 2-(thiophen-2-ylmethylene)malononitrile [125 MHz, $CDCl_3$]

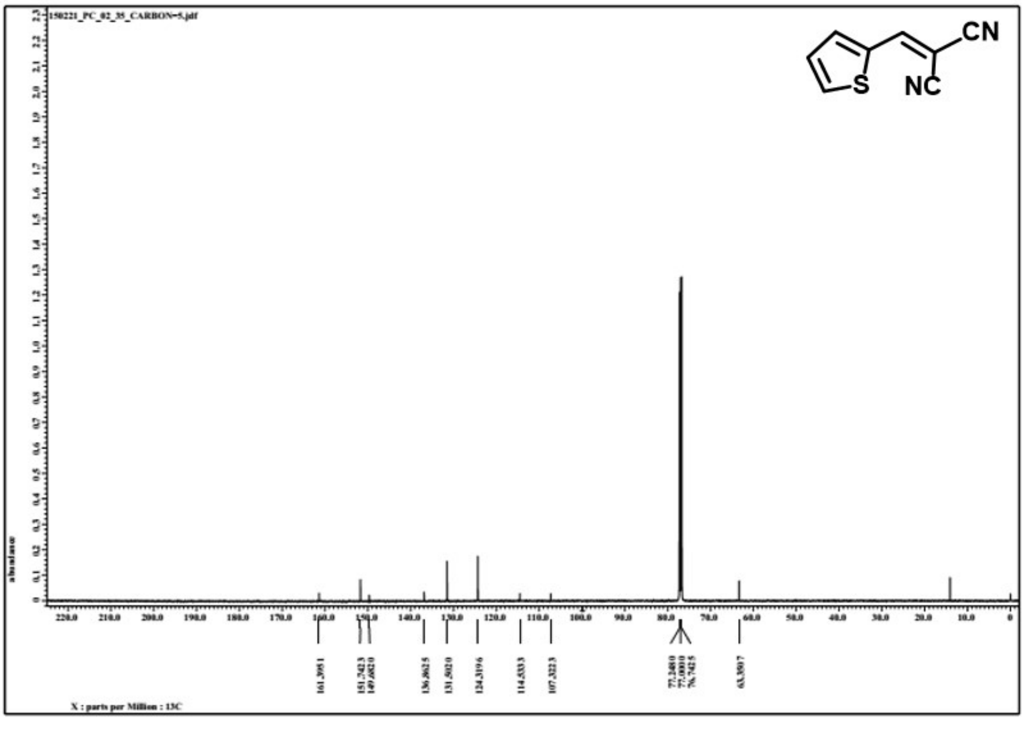

^{1}H-NMR spectra of 3-amino-1-phenyl-1H-benzo[f]chromene-2-carbonitrile

[500 MHz, $CDCl_3$]

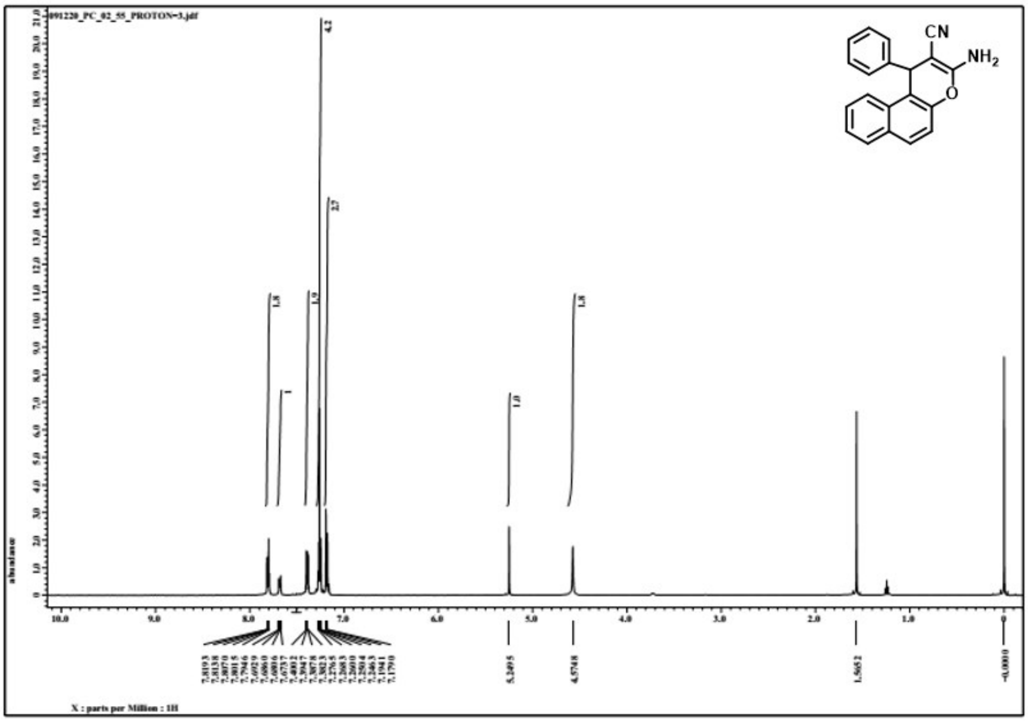

^{13}C-NMR spectra of 3-amino-1-phenyl-1H-benzo[f]chromene-2-carbonitrile

[125 MHz, $CDCl_3$]

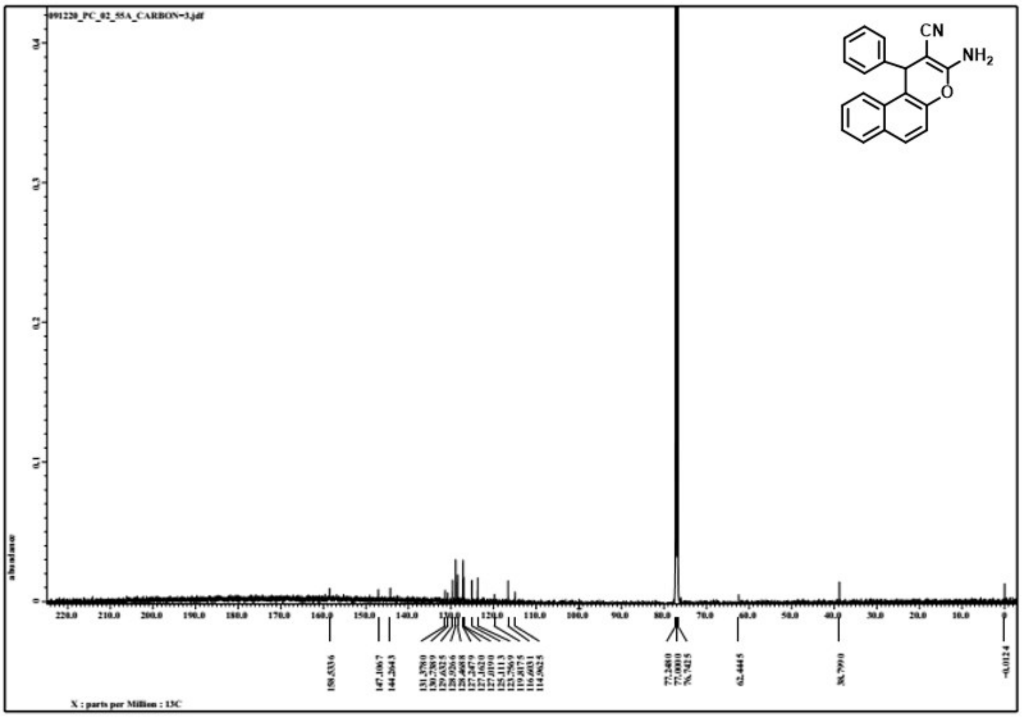

^{1}H-NMR spectra of 3-amino-1-(4-chlorophenyl)-1H-benzo[f]chromene-2-carbonitrile [500 MHz, $CDCl_3$]

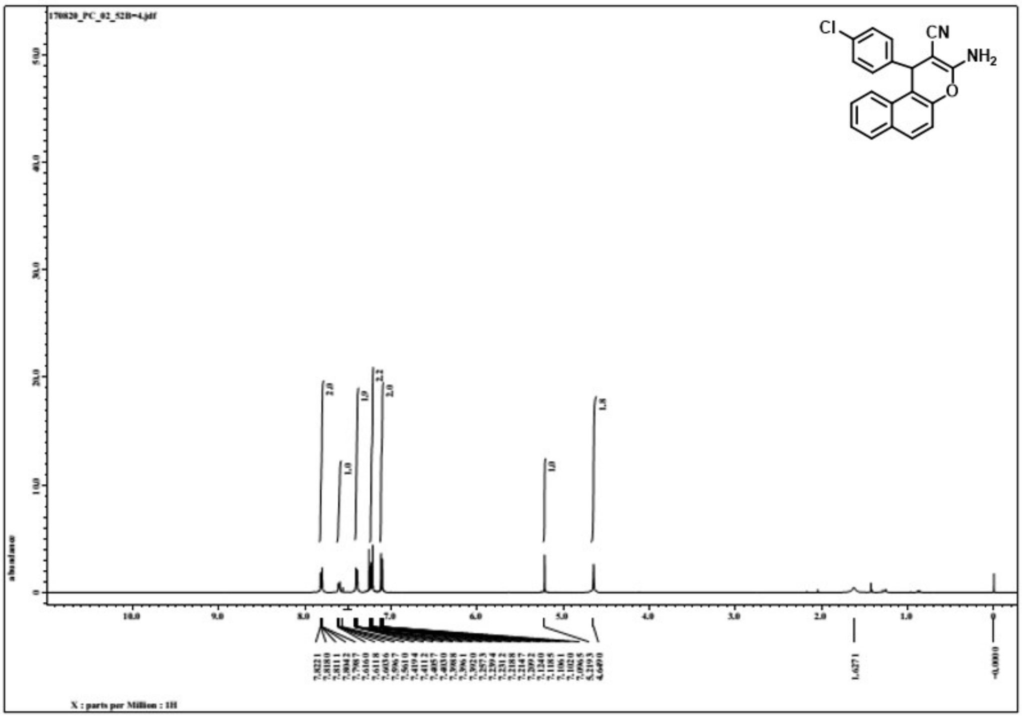

^{13}C-NMR spectra of 3-amino-1-(4-chlorophenyl)-1H-benzo[f]chromene-2-carbonitrile [125 MHz, $CDCl_3$]

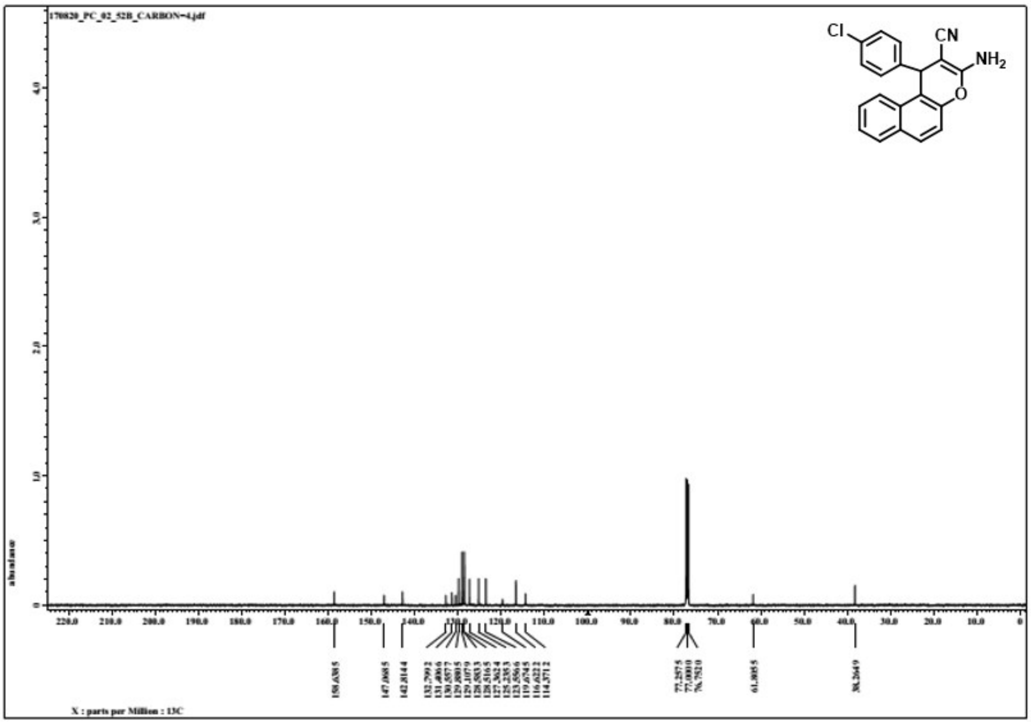

^{1}H-NMR spectra of 3-amino-1-(4-chlorophenyl)-1H-benzo[f]chromene-2-carbonitrile [500 MHz, $CDCl_3$]

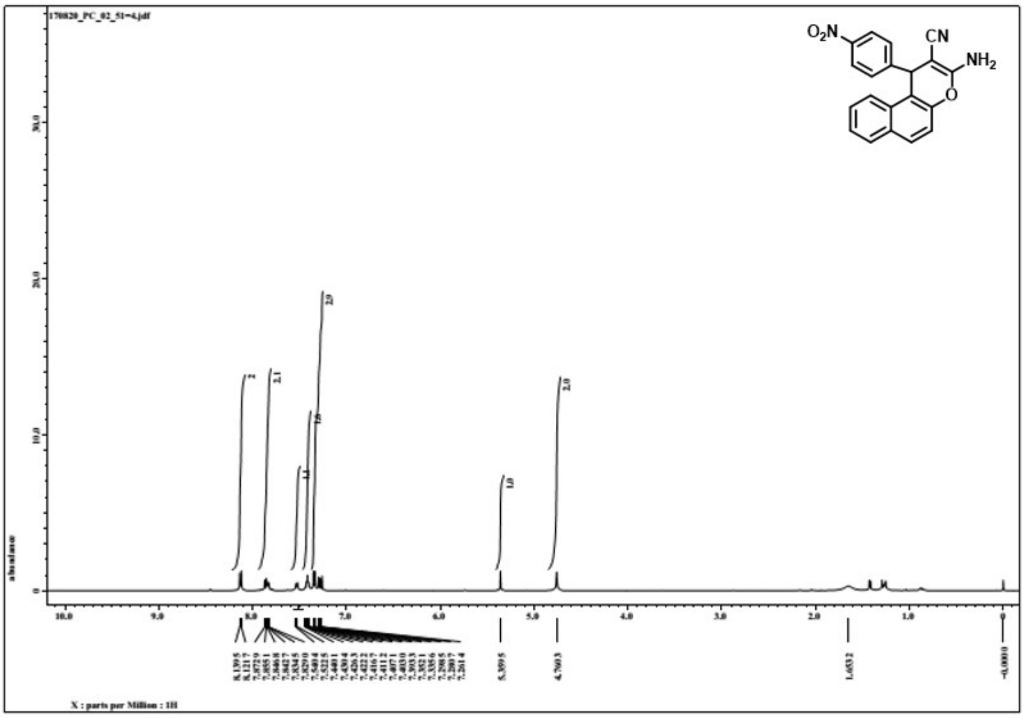

^{13}C-NMR spectra of 3-amino-1-(4-chlorophenyl)-1H-benzo[f]chromene-2-carbonitrile [125 MHz, $CDCl_3$]

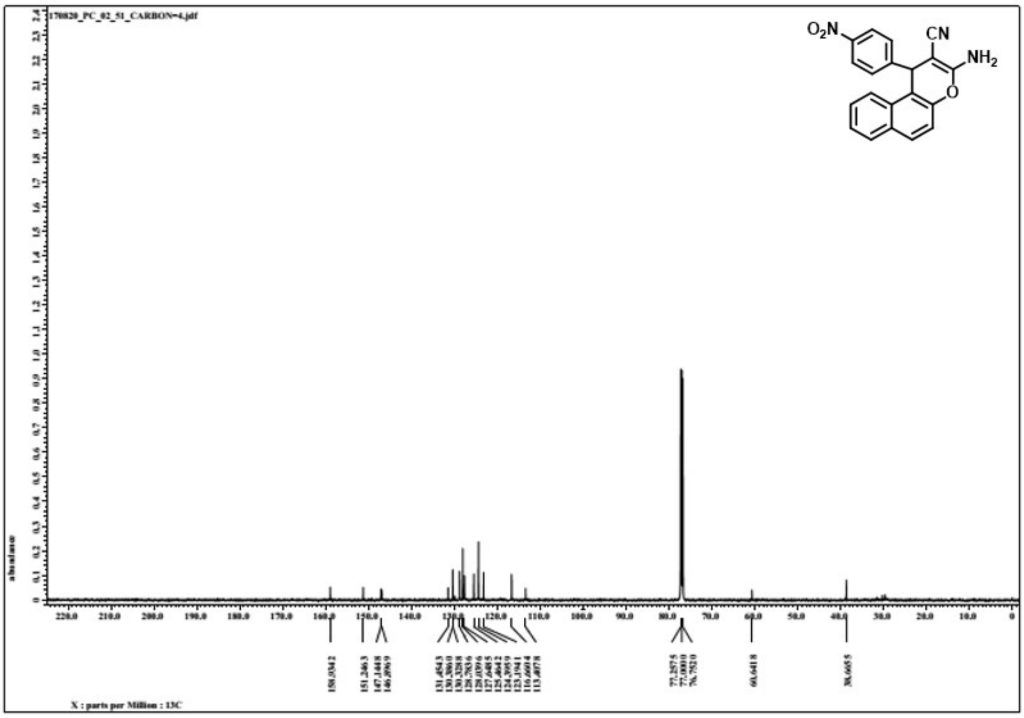

^{1}H-NMR spectra of 3-amino-1-(p-tolyl)-1H-benzo[f]chromene-2-carbonitrile [500 MHz, CDCl$_3$]

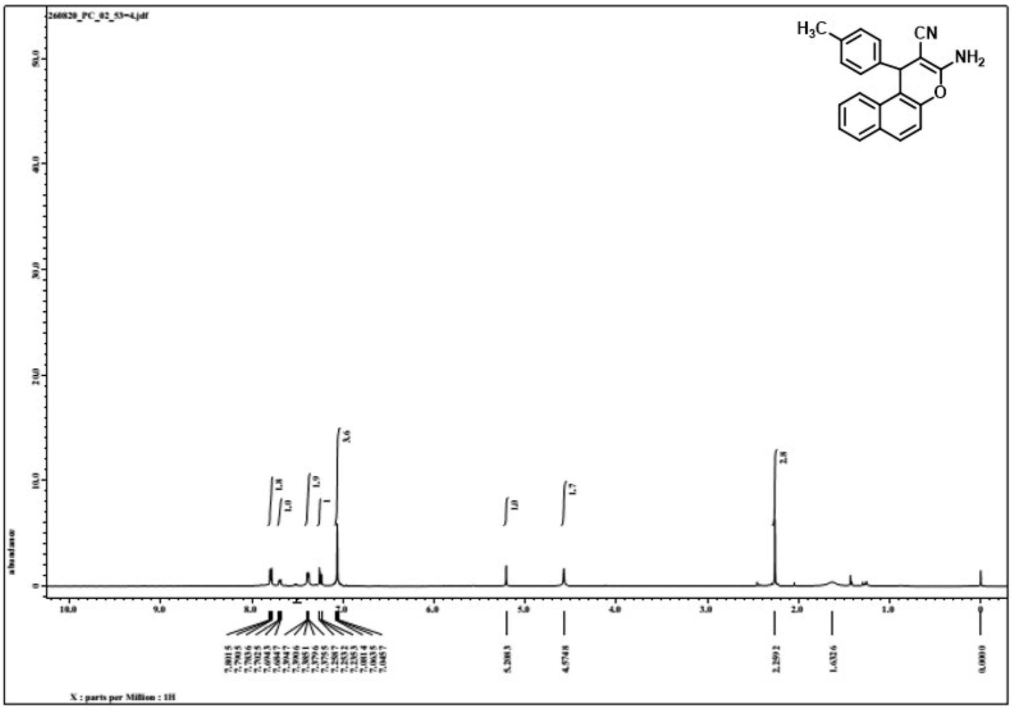

^{13}C-NMR spectra of 3-amino-1-(p-tolyl)-1H-benzo[f]chromene-2-carbonitrile [125 MHz, CDCl$_3$]

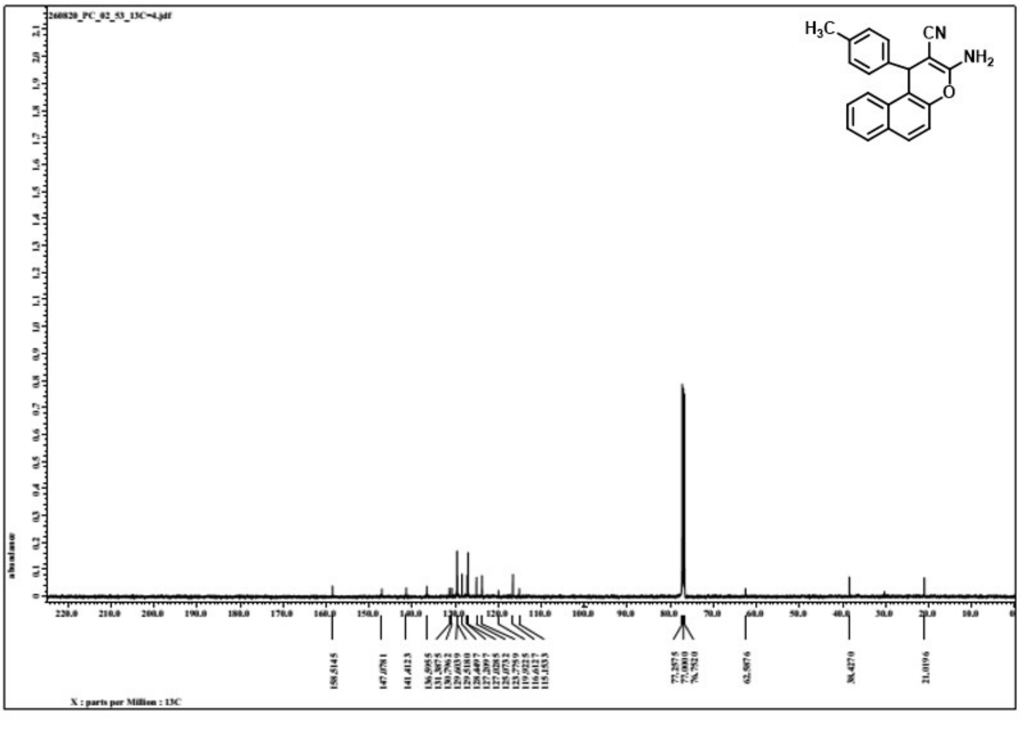

^{1}H-NMR spectra of 3-amino-1-(4-methoxyphenyl)-1H-benzo[f]chromene-2-carbonitrile [500 MHz, $CDCl_3$]

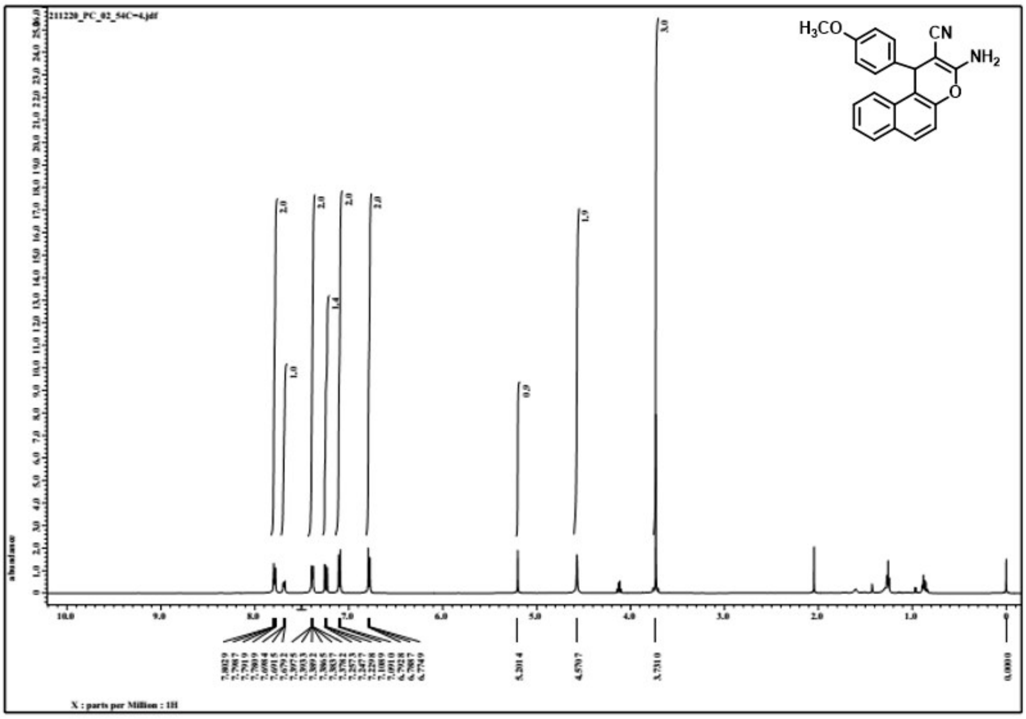

^{13}C-NMR spectra of 3-amino-1-(4-methoxyphenyl)-1H-benzo[f]chromene-2-carbonitrile [125 MHz, $CDCl_3$]

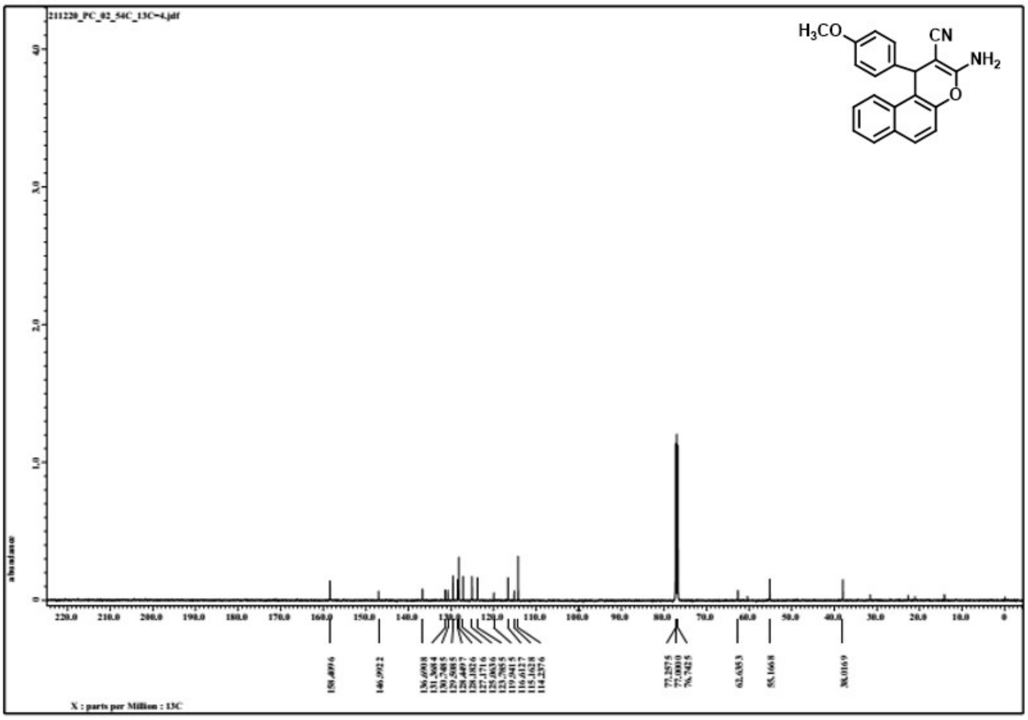

S7. References

1. A. S. Burange, P. S. Tugaonkar, S. D. Thakur, R. R. Khan and R. Shukla, Nano-crystalline $HoCrO_4$: Efficient catalyst for Knoevenagel condensation in water: First catalytic application of Cr (V) species, *Nano-Struct. Nano-Objects*, 2020, **23**, 100493.
2. D. Patel, R. Vithalani and C. K. Modi, Highly efficient FeNP-embedded hybrid bifunctional reduced graphene oxide for Knoevenagel condensation with active methylene compounds, *New J. Chem.*, 2020, **44**, 2868-2881.
3. M. Yousefian and Z. Rafiee, Cu-metal-organic framework supported on chitosan for efficient condensation of aromatic aldehydes and malononitrile, *Carbohydr. Polym.*, 2020, **228**, 115393.
4. H. Tian, S. Liu, Z. Zhang, T. Dang, Y. Lu and S. Liu, Highly Stable Polyoxovanadate-Based Zn–MOF with Dual Active Sites as a Solvent-free Catalyst for C–C Bond Formation, *ACS Sustainable Chem. Eng.*, 2021, **9**, 4660-4667.
5. H. Chen, T. Hu, L. Fan and X. Zhang, One Robust Microporous TmIII–Organic Framework for Highly Catalytic Activity on Chemical CO_2 Fixation and Knoevenagel Condensation, *Inorg. Chem.*, 2020, **60**, 1028-1036.
6. Z.-W. Zhai, S.-H. Yang, Y.-R. Lv, C.-X. Du, L.-K. Li and S.-Q. Zang, Amino functionalized Zn/Cd-Metal–Organic frameworks for selective CO_2 adsorption and knoevenagel condensation reactions, *Dalton Trans.*, 2019, **48**, 4007-4014.
7. C. Srilakshmi, R. Saraf and C. Shivakumara, Structural studies of multifunctional SrTiO3 nanocatalyst synthesized by microwave and oxalate methods: its catalytic application for condensation, hydrogenation, and amination reactions, *ACS omega*, 2018, **3**, 10503-10512.
8. B. Sakthivel and A. Dhakshinamoorthy, Chitosan as a reusable solid base catalyst for Knoevenagel condensation reaction, *J. Colloid Interface Sci.*, 2017, **485**, 75-80.
9. J. B. M. de Resende Filho, G. P. Pires, J. M. G. de Oliveira Ferreira, E. E. Teotonio and J. A. Vale, Knoevenagel Condensation of Aldehydes and Ketones with Malononitrile Catalyzed by Amine Compounds-Tethered $Fe_3O_4@SiO_2$ Nanoparticles, *Catal. Lett.*, 2017, **147**, 167-180.
10. J. Ortiz-Bustos, M. Fajardo, I. del Hierro and Y. Perez, Versatile titanium dioxide nanoparticles prepared by surface-grown polymerization of polyethylenimine for

photodegradation and catalytic C-C bond forming reactions, *Mol. Catal.*, 2019, **475**, 110501.

11. A. Das, N. Anbu, A. Dhakshinamoorthy and S. Biswas, A highly catalytically active Hf (IV) metal-organic framework for Knoevenagel condensation, *Microporous and Mesoporous Mater.*, 2019, **284**, 459-467.
12. H. Zhu, G. Xu, H. Du, C. Zhang, N. Ma and W. Zhang, Prolinamide functionalized polyacrylonitrile fiber with tunable linker length and surface microenvironment as efficient catalyst for Knoevenagel condensation and related multicomponent tandem reactions, *J. Catal.*, 2019, **374**, 217-229.
13. B. Paplal, S. Nagaraju, P. Veerabhadraiah, K. Sujatha, S. Kanvah, B. V. Kumar and D. Kashinath, Recyclable Bi_2WO_6-nanoparticle mediated one-pot multicomponent reactions in aqueous medium at room temperature, *RSC adv.*, 2014, **4**, 54168-54174.
14. P. Das, A. Dutta, A. Bhaumik and C. Mukhopadhyay, Heterogeneous ditopic $ZnFe_2O_4$ catalyzed synthesis of 4 H-pyrans: further conversion to 1, 4-DHPs and report of functional group interconversion from amide to ester, *Green Chem.*, 2014, **16**, 1426-1435.
15. B. Sarmah and R. Srivastava, Highly efficient and recyclable basic ionic liquids supported on SBA-15 for the synthesis of substituted styrenes, carbinolamides, and naphthopyrans, *Mol. Catal.*, 2017, **427**, 62-72.
16. S. Abdolmohammadi, M. Afsharpour and S. Keshavarz-Fatideh, An efficient green synthesis of 3-Amino-1H-chromenes catalyzed by ZnO Nanoparticles thin-film, *S. Afr. J. Chem.*, 2014, **67**, 203–210.
17. D. Tahmassebi, J. E. Blevins and S. S. Gerardot, Zn(L-proline)$_2$ as an efficient and reusable catalyst for the multi-component synthesis of pyran-annulated heterocyclic compounds, *Appl. Organomet. Chem.*, 2019, **33**, 4807.
18. M. P. Lati, F. Shirini, M. Alinia-Asli and M. A. Rezvani, $Fe_3O_4@SiO_2$-Sultone: A Novel and Recyclable Magnetic Nanocatalyst for the Efficient Synthesis of 3, 4 Dihydropyrano [c] Chromenes and 2-Amino-4H-Chromene Derivatives, *J. Nanosci. Nanotechnol.*, 2020, **20**, 973-982.
19. J. Albadi, A. Alihoseinzadeh, A. Mansournezhad and L. Kaveiani, Novel Metal Oxide of CuO-ZnO Nanocatalyst Efficiently Catalyzed the Synthesis of 2-Amino-4 H-chromenes in Water, *Synth. Commun.*, 2015, **45**, 485-493.

20. S. J. Kalita, N. Saikia, D. C. Deka and H. Mecadon, Ni–Al_2O_3 as reusable heterogeneous catalyst for expedient one-pot synthesis of naphthopyrans, *Res. Chem. Intermed.*, 2016, **42**, 6863-6871.

21. S. Sadjadi, M. M. Heravi, V. Zadsirjan and M. Ebrahimizadeh, SBA-15@ methenamine-HPA: a novel, simple, and efficient catalyst for one-pot three-component synthesis of 2-amino-4 H-chromene derivatives in aqueous medium, *Res. Chem. Intermed.*, 2017, **43**, 5467-5483.

22. M. Zendehdel, M. A. Bodaghifard, H. Behyar and Z. Mortezaei, Alkylaminopyridine-grafted on HY Zeolite: Preparation, characterization and application in synthesis of 4H-Chromenes, *Microporous and Mesoporous Mater.*, 2018, **266**, 83-89.

23. A. Khazaee, R. Jahanshahi, S. Sobhani, J. Skibsted and J. M. Sansano, Immobilized piperazine on the surface of graphene oxide as a heterogeneous bifunctional acid–base catalyst for the multicomponent synthesis of 2-amino-3-cyano-4 H-chromenes, *Green Chem.*, 2020, **22**, 4604-4616.

24. R. Teimuri-Mofrad, M. Gholamhosseini-Nazari, E. Payami and S. Esmati, Novel ferrocene-based ionic liquid supported on silica nanoparticles as efficient catalyst for synthesis of naphthopyran derivatives, *Res. Chem. Intermed.*, 2017, **43**, 7105-7118.

25. M. S. Mashhoori, R. Sandaroos and A. Zeraatkar Moghaddam, Highly Proficient Poly Ionic Liquid Functionalized Mn (III) Schiff-Base Catalyst for Green Synthesis of Chromene Derivatives, *ChemistrySelect*, 2020, **5**, 7148-7154.

26. A. Saha, S. Payra and S. Banerjee, On water synthesis of pyran–chromenes via a multicomponent reactions catalyzed by fluorescent t-ZrO_2 nanoparticles, *RSC adv.*, 2015, **5**, 101664-101671.

27. H. Yarahmadi and H. R. Shaterian, Basic magnetic nanoparticles as efficient catalysts for the preparation of naphthopyrane derivatives, *J. Chem. Res.*, 2012, **36**, 49-51.